

Exploring natural genetic variation in photosynthesis-related traits of barley in the field

Yanrong Gao^{1,2}, Merle Stein¹, Lilian Oshana², Wenxia Zhao^{1,5}, Shizue Matsubara^{2,3}, Benjamin Stich^{1,3,4}

¹Institute of Quantitative Genetics and Genomics of Plants, Heinrich Heine University, Düsseldorf, Germany

²IBG-2: Plant Sciences, Forschungszentrum Jülich, Jülich, Germany

³Cluster of Excellence on Plant Sciences (CEPLAS)

⁴Julius Kühn Institute (JKI) – Federal Research Centre for Cultivated Plants, Institute for Breeding Research on Agricultural Crops, Sanitz, Germany

⁵Xinjiang Seed Industry Development Center of China, Urumqi, China.

*Corresponding author: Benjamin Stich

E-mail Yanrong Gao: Yanrong.Gao@hhu.de

Merle Stein: meste109@uni-duesseldorf.de

Lilian Oshana: liesh100@uni-duesseldorf.de

Wenxia Zhao: 827533845@qq.com

Shizue Matsubara: s.matsubara@fz-juelich.de

Benjamin Stich: benjamin.stich@julius-kuehn.de

Highlight

23 field-grown barley inbred lines showed genetic and phenotypic variation in photosynthesis across plant developmental stages, offering possibility for yield enhancement through optimizing photosynthesis via conventional breeding programs.

© The Author(s) 2024. Published by Oxford University Press on behalf of the Society for Experimental Biology.

This is an Open Access article distributed under the terms of the Creative Commons Attribution-NonCommercial-NoDerivs licence (<https://creativecommons.org/licenses/by-nc-nd/4.0/>), which permits non-commercial reproduction and distribution of the work, in any medium, provided the original work is not altered or transformed in any way, and that the work is properly cited. For commercial re-use, please contact reprints@oup.com for reprints and translation rights for reprints. All other permissions can be obtained through our RightsLink service via the Permissions link on the article page on our site—for further information please contact journals.permissions@oup.com.

Abstract

Optimizing photosynthesis is considered an important strategy for improving crop yields to ensure food security. To evaluate the potential of using photosynthesis-related parameters in crop breeding programs, we measured chlorophyll fluorescence along with growth-related and morphological traits of 23 barley inbreds across different developmental stages in field conditions. The photosynthesis-related parameters were highly variable, changing with light intensity and developmental progression of plants. Yet, the variations in photosystem II (PSII) quantum yield observed among the inbreds in the field largely reflected the variations in CO₂ assimilation properties in controlled climate chamber conditions, confirming that the chlorophyll fluorescence-based technique can provide proxy parameters of photosynthesis to explore genetic variations under field conditions. Heritability (H^2) of the photosynthesis-related parameters in the field ranged from 0.16 for the quantum yield of non-photochemical quenching to 0.78 for the fraction of open PSII center. Two parameters, the maximum PSII efficiency in light-adapted state (H^2 0.58) and the total non-photochemical quenching (H^2 0.53), showed significant positive and negative correlations, respectively, with yield-related traits (dry weight per plant and net straw weight) in the barley inbreds. These results indicate the possibility of improving crop yield through optimizing photosynthetic light use efficiency by conventional breeding programs.

Keywords: Barley, chlorophyll fluorescence, crop yields, development, heritability, natural genetic variation, photosynthesis.

List of photosynthesis-related parameters assessed in this study

Parameter	Description
F_v'/F_m'	Maximum efficiency of PSII in light-adapted state
J_{max}	Maximum rate of electron transport
LEF	Linear electron flow
NPQt	Total non-photochemical quenching
Φ_2	Quantum yield of PSII
Φ_{NO}	Quantum yield of non-regulated dissipation processes
Φ_{NPQ}	Quantum yield of non-photochemical quenching
PSII	Photosystem II
qL	Fraction of PSII open center
SPAD	Relative chlorophyll content
TPU	Triose phosphate utilization
$V_{c,max}$	Maximum rate of carboxylation

Accepted Manuscript

Introduction

To satisfy the increasing demands for agricultural products at constant crop production areas, crop yields need to be increased by the year 2050 by about 25%-70% (Hunter *et al.*, 2017). The potential genetic yield under an optimal environment is the product of four main factors: incident solar radiation, light interception efficiency, conversion efficiency, and harvest index (Bonington, 1977). The green revolution led to considerable increases of light interception efficiency and harvest index by introducing dwarfing genes into cereal crops (Hedden, 2003). However, some studies suggest that these two parameters are close to their theoretical maximum in modern crop varieties (e.g., Zhu *et al.*, 2010). Accordingly, crop yield potential may be limited by the remaining bottleneck, the efficiency of light energy conversion by photosynthesis (source limitation) (Long *et al.*, 2006a; Alvarez Prado *et al.*, 2013; Kromdijk and Long, 2016). Thus, enhancing this conversion efficiency has become a breakthrough goal to improve crop yields (Zhu *et al.*, 2010).

Notably, selection of yields might have unintentionally improved the conversion efficiency, as indicated by a positive relationship between photosynthesis and crop yields (Kromdijk and Long, 2016; Theeuwens *et al.*, 2022). Still, the conversion efficiency has not reached the theoretical maximum in C₃ plants (Long *et al.*, 2006b; Zhu *et al.*, 2010; Prosekov and Ivanova, 2018) after decades of selection for crop yields. This suggests that the selection for yields is not sufficient to fully explore and make better use of natural genetic variation of photosynthesis. Direct phenotyping and selection for photosynthesis parameters are needed to identify variations in photosynthetic capacity and source limitation of crop yield (Theeuwens *et al.*, 2022).

Several studies have successfully increased yields through optimizing photosynthesis by genetic engineering (reviewed by Simkin *et al.*, 2019), such as manipulating the Calvin–Benson cycle in wheat (Driever *et al.*, 2017), carbon transport in rice (Gong *et al.*, 2015) and soybean (Hay *et al.*, 2017), or photoprotection in tobacco (Kromdijk *et al.*, 2016) and in soybean (De Souza *et al.*, 2022). However, the use of genetically modified crops is restricted in some parts of the world (Turnbull *et al.*, 2021) and suggested yield improvements by the genetic modifications await

rigorous tests in practical agricultural production conditions (Khaipho-burch *et al.*, 2023). Classical breeding can offer an alternative or an additional approach. Indeed, natural variation of photosynthesis within (Wullschleger, 1993) and across species (Flood *et al.*, 2011; van Bezouw *et al.*, 2019; Garcia *et al.*, 2022) can be exploited by classical breeding.

Natural genetic diversity of photosynthesis has been studied in cereals under field conditions. Driever *et al.* (2014) reported significant variations in photosynthetic capacity, biomass and yield in 64 wheat genotypes. Acevedo-Siaca *et al.* (2021a) observed high heritabilities for carbon assimilation-related parameters in 30 accessions of rice. However, the relationships between photosynthesis and yields observed in these studies were not consistent. For example, Carmo-Silva *et al.* (2017) observed a positive correlation between carbon assimilation rate and grain yields in field-grown wheat in pre- and post- anthesis stage, while Driever *et al.* (2014) found no correlation between carbon assimilation-related parameters and grain yield in field-grown wheat in pre-anthesis stages. A possible explanation for such discrepancies may be the dependency of the photosynthetic traits on environmental conditions and/or developmental stages of the plants, although further research is needed to clarify this. Furthermore, in barley, one of the most important cereal crops as well as a model for other cereals because of its simpler genetics, natural variation of photosynthesis has not been investigated under field conditions.

High-throughput phenotyping techniques are essential for investigating the natural genetic variation in photosynthesis. Photosynthesis is divided into two main processes, light reaction and CO₂ assimilation, which can be assessed by chlorophyll fluorescence- and gas exchange-based techniques, respectively (Long *et al.*, 1996; Baker, 2008). The analysis of chlorophyll fluorescence provides information on photosystem II (PSII) activity, such as the effective and the maximum quantum yields of PSII (Φ_2 and F_v'/F_m' , respectively, for light-adapted state) or non-photochemical quenching (NPQ) (Baker, 2008). Measurement of gas exchange allows estimation of carbon assimilation rate (A) and related parameters (Sharkey, 2016). Recently, dynamic assimilation technique (DAT) was introduced to enable gas exchange measurements in non-steady state, which substantially increased the throughput compared to steady-state measurements (Saathoff and Welles, 2021) albeit still slower than chlorophyll fluorescence-

based methods. For applications to crop breeding and selection, it is essential to check whether the genetic variations detected by these two techniques are comparable or not.

The objectives of this study were to 1) investigate genetic variation of photosynthesis-related parameters in barley across different developmental stages and evaluate the interaction between genotypes and environment in field conditions, 2) compare gas exchange- and chlorophyll fluorescence-based assessments of photosynthetic traits, and 3) assess correlation between photosynthesis-related and morphological or growth-related parameters. Based on the results obtained, we will consider the potential of using photosynthesis-related parameters in crop and particularly barley breeding programs.

Materials and methods

Field experimental design

Twenty-three spring barley (*Hordeum vulgare*) inbreds were selected from a world-wide collection of 224 barley landraces and cultivars based on their genetic and phenotypic diversity (Weisweiler *et al.*, 2019). These 23 barley inbreds are the parents of the double round-robin population (Casale *et al.*, 2022). All 23 inbreds were grown at three different locations (Bonn (50°37'31.82" N 6°59'18.508" E), Cologne (50°57'34.345" N 6°51'36.407" E), and Düsseldorf (51°10'42.599" N 6°48'8.268" E) in Germany in 2021. In Bonn, the experimental design was an alpha design with two complete replications, where the plants were sown in 10 m^2 plots on March 31. In Düsseldorf, the experimental design was an alpha design with three complete replications. The experimental unit were single rows with 33 kernels per row and six rows together were considered as one plot (replicate). The plants in Düsseldorf were sown on March 31. In Cologne, two distinct trials were performed, which were named in the following as "mini-big plot" and "big plot" trials. Within each of these two trials, 23 inbreds were grown as replicated checks in an augmented design. In the mini-big plot trial, each plot had a size of 2.25 m^2 . The entire mini-big plot trial had 320 plots, in which the 23 inbreds were grown as replicated checks twice. The big plot trial, in which each plot had a size of 10 m^2 , comprised also 320 plots and the

23 inbreds were also grown as checks but only one time. Fertilization and crop protection followed local practices. Air temperature and precipitation were recorded during the field experiments at all three locations (Supplementary Fig. S1). In Bonn, the field site has chernozem-para-brown soil, and the field sites, in Cologne and Düsseldorf, have para-brown soil (Bundesanstalt für Geowissenschaften und Rohstoffe (BGR)).

Climate chamber experimental conditions and design

Based on the results of the field experiments, six representative barley inbreds (HOR1842, IG128216, IG31424, ItuNative, K10877, and W23829/803911) were selected for a climate chamber experiment. The experimental design was a randomized complete block design with three replicates/blocks. A total of 32 plants were planted for each inbred in total. The gas exchange measurements were performed 21, 24, 26, 31, 36, 39, 46, 51, 57, 74, 87, 88, 100, and 102 days after sowing (DAS). At each measurement day, three measurements were taken from three different plants of an inbred, where always one plant from each of the blocks was studied. In addition, the Zadoks score for each evaluated plant was rated. In addition, we harvested three plants per inbred (i.e. one per block) and then measured dry weight of above ground biomass per plant 26, 36, 46, 57, 74, 102, 113, and 142 DAS. The growth conditions in the climate chamber were as follows: 14 h/10 h light/dark photoperiod, 18°C/16°C temperature, and 55% relative humidity. The maximal light intensity measured at 15 cm from the light panel was $750 \mu\text{mol m}^{-2} \text{s}^{-1}$.

Assessment of photosynthesis-related parameters

In the field experiments, the top fully expanded leaves of three representative plants from each plot were measured from seedling stage (ZS13, (Zadoks *et al.*, 1974)) to dough development (ZS87) using MultispeQ V2 device (Kuhlgert *et al.*, 2016). We used the measurement protocol “Photosynthesis RIDES”, by which the intensity of actinic light was automatically set to the ambient light intensity measured by the built-in light sensor. The following parameters were used for the further analyses: linear electron flow (LEF), the fraction of open PSII centers (qL), the quantum yield of PSII (Phi2), the maximum efficiency of PSII in light-adapted state (F_v'/F_m'), the

total NPQ (NPQt), the quantum yield of NPQ (PhiNPQ), the quantum yield of non-regulated dissipation processes (PhiNO), and relative chlorophyll content (SPAD). In addition, the MultispeQ also recorded environmental parameters, such as the intensity of photosynthetically active radiation (PAR), ambient temperature, ambient humidity, and ambient pressure.

In the climate chamber experiment, parameters of gas exchange were measured multiple times from tillering stage (ZS21) to dough development (ZS89) alongside the MultispeQ measurements. The measurements were made on the top fully expanded leaves on the main stem. Three different light intensities (PAR = 400, 800, 1500 $\mu\text{mol m}^{-2}\text{s}^{-1}$) were used as simulated low-light (LL), medium-light (ML) and high-light (HL) conditions for the MultispeQ measurements. Leaf-level gas exchange measurements were performed by LI-6800 (LI-COR Biosciences Inc., Lincoln). Three replicates per genotype were measured from 1 h after the onset of the light period. The settings inside the LI-6800 chamber were as follows: PAR was kept at 1500 $\mu\text{mol m}^{-2}\text{s}^{-1}$ (as in the simulated HL) with 50% blue and 50% red light, 400 $\mu\text{mol s}^{-1}$ air flow rate, 10,000 rpm fan speed, 55% relative humidity, and 18°C air temperature. The proportion of blue and red light was chosen to mimic the HL conditions in the field. The humidity and air temperature in the LI-6800 chamber were chosen to mimic the growth condition in the climate chamber and, thus, reduce the time needed for stabilization prior to the measurements. The CO₂ concentration inside the LI-6800 chamber was 400 ppm during pre-acclimation which lasted between 10 and 15 min. After the pre-acclimation, photosynthetic CO₂ response (A/C_i) curves were measured according to DAT (Saathoff and Welles, 2021). CO₂ ramps were started from 1605 to 5 ppm with ramping rates of 200 ppm. The A/C_i curves were then analyzed using the “plantecophys” package (Duursma, 2015) in R version 4.0.3 to estimate the maximum rate of carboxylation ($V_{c,max}$), the maximum rate of electron transport (J_{max}), and triose phosphate utilization (TPU).

Assessment of morphological and growth-related traits

To determine the relative growth rate (RGR) of the 23 barley inbreds, aboveground biomass data were collected in the field experiment in Düsseldorf at six different time points during the vegetation period: at 62, 69, 76, 83, 97, and 125 DAS. Plants of one row (initially 33 kernels were

sown) per plot were harvested for the 23 genotypes with three replicate plots. Wild animals visited the trails and, thus, the number of damaged plants for each row was recorded.

The dry weight per row per plot was used to estimate the dry mass per plant (DMP), which was needed for the assessment of growth curve parameters, using the following equation:

$$DMP = \frac{DM}{(TNP - NDP) + 0.8 \times NDP} \quad (1)$$

where TNP was the total number of plants, NDP the number of damaged plants, 0.8 was the completeness of the damaged plants based on the observation during the harvest. DMP calculated as described above, was corrected separately for each time point for replicate and block effects. The corrected values were then used for further analyses.

In the climate chamber experiment, the total aboveground DMP was measured by weighing at eight different time points (26, 36, 46, 57, 74, 102, 113, and 142 DAS) except for the two inbreds IG31424 and HOR1842, for which only the initial and the final DMP were determined at 26 and 142 DAS. Three replicates per genotype were collected for each time point.

To assess the relationship between DMP and time, logistic (Verhulst, 1838), power-law (Paine *et al.*, 2012), and quadratic regression (Lithourgidis and Dordas, 2010) models were fitted. The quadratic regression model was used:

$$y_r = a + bt - ct^2 \quad (2)$$

where a represents the initial biomass, b and c the growth rate parameters. This model had a high coefficient of determination (R^2) and the highest heritability across all 23 barley inbreds. Thus, the quadratic regression was used for estimation of RGR. RGR_a , RGR_b , RGR_c represent the parameters in quadratic regression a , b , and c , respectively.

Morphological parameters were collected in multi-year and multi-environment field experiments that took place in the years 2017-2021 at Düsseldorf, Cologne, Mechernich, and Quedlinburg (Wu *et al.*, 2022; Shrestha *et al.*, 2022). Not all locations were used in all years to assess all parameters. Flag leaf length (FL, cm) and width (FW, cm), plant height (PH), flowering time (FT), awn length (AL, cm), spike length (EL, cm), and spikelet number in one row of the spike (SR), seed length (SL,

mm), seed width (SW, mm), seed area (SA, mm²), and thousand grain weight (TGW, g), grain weight (GW, Kg/10 m²), and net straw weight (NSW, Kg/10 m²) were measured as morphological parameters. FL, FW, AL, EL were measured by ruler, SL, SW, and SA were measured by MARViN seed analyser (MARViNTECH GmbH, Germany), TGW was measured by MARViN and a balance.

The same set of morphological parameters was also measured in the climate chamber experiment. FL and FW were collected at 74 and 102 DAS with three replicates, and spike-related traits (AL, EL, SR, SL, SW SA, and TGW) were collected at 142 DAS with three replicates. Additionally, the total stem (without spike) weight per plant (SWP, g), total spike weight per plant (SKWP, g), total stem weight of main stem (TSWM, g), and spike weight of main stem (SKWM, g) were also collected in the climate chamber experiment. Harvest index (HI) was calculated using the following equation:

$$HI = \frac{SWP}{DMP} \quad (3)$$

In addition, harvest index of main stem (MSHI) was calculated using the following equation:

$$MSHI = \frac{MSW}{TMSW} \quad (4)$$

Statistical analyses

Field experiment

Due to the strong dependence of photosynthesis on light intensity (Ogren, 1993), we considered three light intensity clusters when analyzing field measurements: LL, ML and HL conditions. These light intensity clusters were identified by K-means clustering of PAR and LEF. In addition, we also compared three main developmental phases of barley, i.e., slow expansion phase (SEP) (ZS<30), rapid expansion phase (REP) (30≤ZS<60), as well as anthesis and senescence phase (ASP) (ZS≥60). These two factors light intensity (L) and developmental phase (S), each with three levels, were considered when analysing the MultispeQ parameters from the field experiments based on the following linear model with the quantitative covariates light intensity (PAR) and developmental stage (ZS):

$$y_{(p)ijklmnopqr} = \mu + G_i + E_j + (G:E)_{ij} + ZS_k + L_l + S_m + (G:L)_{il} + (G:S)_{im} + M_n + D_o \\ + PAR_{ijklmnopqr} + T_{ijklmnopqr} + (E:R)_{jp} + (E:R:B)_{j pq} + \epsilon_{(p)ijklmnopqr}$$

(5)

where $y_{(p)ijklmnopqr}$ was the observed MultispeQ parameter across all light conditions and all developmental stages, μ the general mean, G_i the effect of the i^{th} inbred, E_j the effect of the j^{th} environment, $(G:E)_{ij}$ the interaction between the i^{th} inbred and the j^{th} environment, ZS_k the effect of k^{th} Zadoks score of barley development, L_l the effect of l^{th} light intensity cluster, S_m the effect of m^{th} barley developmental phase, $(G:L)_{il}$ the interaction between i^{th} inbred and l^{th} light intensity cluster, $(G:S)_{im}$ the interaction between i^{th} inbred and m^{th} barley developmental phase, M_n the effect of the n^{th} MultispeQ device, D_o the effect of measurement date, $(E:R)_{jp}$ the effect of the p^{th} replicate nested within j^{th} environment, $(E:R:B)_{j pq}$ the effect of the q^{th} block nested within the p^{th} replicate in j^{th} environment, $PAR_{ijklmnopqr}$ the light intensity of each measurement, $T_{ijklmnopqr}$ the ambient temperature of each measurement, and $\epsilon_{(p)ijklmnopqr}$ the random error.

To estimate adjusted entry means for MultispeQ parameters of all inbreds, G_i , E_j , $(G:E)_{ij}$, ZS_k , L_l , S_m , $(G:L)_{il}$, and $(G:S)_{im}$ were treated as fixed effects, and M_n , D_o , $(E:R)_{jp}$, $(E:R:B)_{j pq}$ as random effects, $PAR_{ijklmnopqr}$ and $T_{ijklmnopqr}$ were covariates. Furthermore, we calculated adjusted entry means for all inbreds for each light intensity cluster as well as each developmental phase.

In addition, to evaluate the effect of each fixed factor and covariate, analysis of variance (ANOVA) was conducted.

To assess the heritability of each photosynthesis-related parameter at each developmental stage, which was considerably shorter than the above-mentioned three developmental phases, data were separated into eight stages from Zadoks principal growth stages. The adjusted entry means were calculated based on the following model:

$$y_{(pd)ijlnopqr} = \mu + G_i + E_j + M_n + D_o + PAR_{ijklmnopqr} + T_{ijklmnopqr} \\ + (E:R)_{jp} + (E:R:B)_{j pq} + \epsilon_{(p)ijklmnopqr}$$

(6)

where, $y_{(pd)ijklmnopqr}$ was the photosynthesis-related parameter for each developmental stage across all other factors. Due to convergence problems, the interaction between G_i and E_j was removed from this model.

To assess the similarities among the barley genotypes with respect to their photosynthesis parameters, we performed hierarchical clustering by Ward's minimum variance theory (Ward Jr, 1963) using the adjusted entry means of PSII parameters and SPAD at three different developmental phases. Furthermore, principal component analysis (PCA) was conducted by using the adjusted entry means calculated for each inbred in each of the developmental phases described before. In addition, a PCA was conducted by using the environmental factors (temperature and precipitation) of the inbreds at the country of origin. The relationship between photosynthesis-related parameters and morphological or growth-related parameters of the inbreds was evaluated by Pearson correlation coefficients among adjusted entry means.

Climate chamber experiment

The adjusted entry means of carbon assimilation-related parameters from the climate chamber experiment were calculated based on the following model:

$$y_{(A)ijklmr} = \mu + G_i + ZS_j + D_k + (D:TW)_{kl} + S_m + (G:S)_{im} + \epsilon_{(A)ijklmr} \quad (7)$$

where $y_{(A)ijklmr}$ was the carbon assimilation-related parameter, $D:TW_{kl}$ the effect of the l^{th} time window in the k^{th} date of measurement, and $\epsilon_{(A)ijklmr}$ the random error. To estimate adjusted entry means for carbon assimilation-related parameters of six barley inbreds, G_i , ZS_j , S_m and $(G:S)_{im}$ were treated as fixed effects, as well as D_k and $D:TW_{kl}$ as random effects.

The relationship between photosynthesis-related parameters and morphological or growth-related parameters of the inbreds was evaluated by Pearson correlation coefficients between adjusted entry means.

Estimation of heritability

Broad-sense heritability (H^2) was estimated for both field and climate chamber experiments based on the following method:

$$H^2 = \sigma_G^2 / (\sigma_G^2 + \bar{v}_\delta^{BLUE} / 2) \quad (8)$$

where σ_G^2 was the genotypic variance calculated based on the above models with a random effect for G_i and \bar{v}_δ^{BLUE} was the mean variance of the difference of two genotypic means (Holland *et al.*, 2003; Piepho and Möhring, 2007).

To avoid the effect of the varying number of replicates, the H^2 of photosynthesis-related parameters was estimated for each developmental stage based on the following equation:

$$H^2 = \sigma_G^2 / (\sigma_G^2 + \sigma_{G:E}^2 / 5 + \sigma_e^2 / 5) \quad (9)$$

where $\sigma_{G:E}^2$ was the variance of the interaction of barley inbreds and environments, and σ_e^2 was the residual variance.

We used the statistical software R to perform all statistical analyses.

Results

Factors affecting photosynthesis-related parameters in the field

Parameters of PSII and SPAD were collected under field conditions with a wide range of PAR from 67 to 2172 $\mu\text{mol m}^{-2}\text{s}^{-1}$. In general, LEF increased as PAR increased, with an increasing variability among the individual observations at higher PAR (Fig. 1A). An increase of PAR was associated with a decrease of Phi2 and an increase of PhiNPQ, while PhiNO remained relatively stable (Supplementary Fig. S2A-C). Note that the sum of Phi2, PhiNPQ and PhiNO is equal to one. The light-dependent changes in Phi2 were accompanied by the corresponding changes in F_v'/F_m' and qL (Supplementary Fig. S2D, E). The light response of NPQt was similar to that of PhiNPQ except that it often gave extreme values (Supplementary Fig. S2F). In contrast to these PSII parameters, SPAD values were not affected by momentary PAR (Supplementary Fig. S2G).

Given the strong influence of PAR on PSII parameters, K-means clustering was performed to separate the observations of LEF into three groups based on the light intensity: LL, ML, and HL conditions (Fig. 1B). As expected, significant ($P < 0.05$) differences in Phi2 and PhiNPQ, but not SPAD, were observed among the three light intensities (Fig. 2A). We then assessed the impact of developmental phase on these parameters: SEP, REP, and ASP (Fig. 2B). All three parameters showed significant ($P < 0.05$) differences between SEP and REP; Phi2 and SPAD increased from SEP to REP while PhiNPQ decreased (Fig. 2B). Thus, both PAR and developmental phases seem to affect Phi2 and PhiNPQ, whereas SPAD changed with plant development.

Significant ($P < 0.05$) effects on PSII parameters and SPAD were observed for the interactions between genotype and environment ($\sigma_{G:E}^2$), genotype and light condition ($\sigma_{G:L}^2$) and genotype and developmental phase ($\sigma_{G:S}^2$), along with the effects of genetic variation (σ_G^2) or other variables such as the date of measurement (σ_D^2), the used MultispeQ device (σ_M^2), and the replicate ($\sigma_{E:R}^2$) (Table 1). Analysis of variance also confirmed significant ($P < 0.05$) effects of PAR, light condition, developmental phase, and developmental stage (rated on the Zadoks scale) on the different PSII parameters and SPAD (Table 2). In addition, ambient temperature (T), which typically covaries with light intensity in the field, also significantly ($P < 0.05$) affected the PSII parameters except PhiNPQ in barley.

Genetic variations in photosynthesis-related traits

When data from all light conditions and all developmental stages were combined together, H^2 of the examined parameters ranged between 0.16 (PhiNPQ) and 0.78 (qL) (Table 1). Notably, when the heritability was calculated separately at different developmental stages as defined by Zadoks growth scale, the H^2 values of these parameters were considerably lower in the seedling growth stage and significantly ($P < 0.05$) higher in the dough developmental stage (Supplementary Fig. S3). In accordance, all PSII parameters and SPAD had low H^2 values in the slow expansion phase (SEP) (Fig. 3). In the rapid expansion phase (REP), SPAD and Phi2 had the highest H^2 while NPQt and Fv'/Fm' had the lowest. In anthesis and senescence phase (ASP), the H^2 of Phi2 decreased dramatically.

Hierarchical cluster analysis of the adjusted entry means of the PSII parameters and SPAD observed in each of the three developmental phases indicated the presence of four major clusters among the 23 barley inbred lines (Fig. 4A). In general, the four clusters differed in the PSII parameters but not in SPAD (Fig. 5A). All PSII parameters except NPQt showed significant ($P < 0.05$) differences among the four clusters in each of the three developmental phases (Fig. 5A).

We then asked whether the four clusters also represented differences in growth-related and morphological parameters among the 23 inbred lines. Relative growth rates (RGR) were calculated from the changes in DMP in the field experiment in Düsseldorf (Supplementary Fig. S4). Based on the growth parameters alone, the inbred lines could be divided into two clusters by hierarchical cluster analysis: DMP remaining at the same level after 100 days after sowing, and DMP increasing throughout the entire growth season (Supplementary Fig. S4). We observed no significant difference ($P = 0.3$) in flowering time between the two groups. When PCA was performed on a combination of the PSII parameters and SPAD data shown in Fig. 2 as well as the growth-related parameters derived from Supplementary Fig. S4 and morphological traits collected from multi-year and multi-environment field experiments, the analysis revealed four clusters (Fig. 4B) that were very similar to those identified based on the PSII parameters and SPAD alone (Fig. 4A). Comparing the four clusters, we found no significant difference in DMP and RGR (Fig. 5B) or the morphological traits (Supplementary Fig. S5). Moreover, no significant correlation was observed between the first two principal components and the environmental information of the inbreds' country of origin (Fig. 4C). Together, these results suggest that the clustering of the inbreds according to photosynthetic parameters primarily reflects genetic variations in photosynthetic traits among the 23 inbreds and is not confounded by differences in growth-related and morphological parameters.

Comparison of gas exchange-based parameters and PSII parameters

Of the 23 barley inbreds, six (HOR1842, IG128216, IG31424, ItuNative, K10877, and W23829/803911) were selected to assess carbon assimilation-related parameters in climate chamber conditions. These six inbreds differed in the PSII parameters and SPAD assessed in the

field. HOR1842 had the lowest adjusted entry means for Phi2, qL, and SPAD, IG128216 had the highest Phi2 and LEF. IG31424 had the highest PhiNPQ and the lowest SPAD. ItuNative had the lowest SPAD with relatively high Phi2, whereas K10877 had the highest SPAD with average values of PSII parameters. W23829/803911 was characterized by the lowest PhiNPQ and NPQt.

The gas exchange measurements in the climate chamber resulted in high H^2 values for carbon assimilation-related parameters, ranging between 0.820 and 0.895 (Table 3). We observed a significant genetic variation ($P < 0.05$) for carbon assimilation at saturating light intensity (A_{sat}) among the six inbreds (Fig. 7A); the adjusted entry means of A_{sat} were ranging from 14.7 (IG31424) to 19.7 (K10877) $\mu\text{mol m}^{-2}\text{s}^{-1}$. The differences in the maximal carboxylation ($V_{c,max}$) and electron transport rates (J_{max}) as well as triose phosphate utilization capacity (TPU) were also significant ($P < 0.05$) among the six inbreds (Fig. 7A). Similarly, Phi2 (measured at LL, ML and HL) and SPAD showed significant ($P < 0.05$) differences among the six inbreds (Fig. 7B). Carbon assimilation-related parameters underwent significant ($P < 0.05$) changes across the developmental phases, all peaking in REP together with Phi2 and SPAD (Fig. 7C, D). The H^2 values for the PSII parameters and SPAD were also generally high, including 0.92 for Phi2 and 0.96 for SPAD (Table 3).

We observed significant ($P < 0.05$) positive correlations between SPAD, Phi2 and LEF (both measured at HL) and all four carbon assimilation-related parameters (determined at HL) in the climate chamber (Fig. 8). As anticipated, PhiNPQ and NPQt were negatively correlated with the four carbon assimilation-related parameters.

The adjusted entry means of the six barley inbreds showed significant ($P < 0.05$) positive correlations between Phi2 and carbon assimilation-related parameters in the climate chamber experiment (Fig. 9). In comparison, the correlations between these parameters assessed in the climate chamber experiment and Phi2 observed in the field were lower, with the highest correlation coefficient of 0.72 found for Phi2 at HL between these experiments.

Relationship between photosynthesis-related parameters and growth or morphological parameters

Morphological parameters and DMP were determined in the climate chamber experiment to assess the relationship between the photosynthesis-related parameters and morphological or growth-related parameters. As done for the field experiments (Supplementary Fig. S4), RGR was calculated for the six inbred lines by fitting a quadratic regression to the DMP data (Supplementary Fig. S7). No significant correlation was observed between the morphological traits, DMP-based RGR and photosynthesis-related parameters among the six barley inbreds (Fig. 8).

We then made the same analysis using the data from the 23 inbred lines in the field experiments (Fig. 6). As expected, we found significant ($P < 0.05$) positive or negative correlations among the PSII parameters as well as among the growth-related parameters. No significant correlation was observed between SPAD and all PSII parameters when the adjusted entry means of all developmental stages and locations were considered (Fig. 6). Comparing the PSII parameters and the growth-related parameters, the final DMP was significantly ($P < 0.05$) positively and negatively correlated with F_v'/F_m' and NPQt, respectively. RGR_c showed a significant ($P < 0.05$) positive correlation with NPQt (Fig. 6). Looking at the PSII parameters and morphological traits collected from multiple environments and years, significant ($P < 0.05$) positive correlations were observed between two PSII parameters (Φ_{iNO} and F_v'/F_m') and NSW (Fig. 10). In addition, significant negative correlations were observed between three PSII parameters (q_L , NPQt, Φ_{iNPQ}) and NSW. Φ_{i2} , LEF and q_L were significantly ($P < 0.05$) negatively correlated with flag leaf morphology (FL and FW) (Fig. 10).

Discussion

Comparison of chlorophyll fluorescence- and gas exchange-based techniques.

In order to assess the genetic variation of photosynthesis-related parameters in breeding programs, high-throughput methods are needed. Chlorophyll fluorescence-based techniques and hyperspectral measurement techniques have the potential to serve as high-throughput

methods to evaluate photosynthetic traits (for review see van Bezouw et al., 2019). Hyperspectral sensing techniques rely on indirect correlations between features of reflectance spectra and photosynthesis. Once such correlations have been characterized, they can be used to predict photosynthesis capacity at plot- (Meacham-Hensold *et al.*, 2019) or leaf-level (Serbin *et al.*, 2011; Ainsworth *et al.*, 2014; Yendrek *et al.*, 2016; Silva-Perez *et al.*, 2017). However, compared to chlorophyll fluorescence- and gas exchange-based techniques, reflectance spectra are less sensitive to short-term changes in photosynthesis. Furthermore, correlation-based prediction models cannot be readily applied to new genetic materials, especially across different years and different environmental conditions (Meacham-Hensold *et al.*, 2019). Hence, gas exchange- and chlorophyll fluorescence-based techniques, particularly the latter for high-throughput measurements, are considered more reliable and straightforward to explore genetic diversity of photosynthesis and related traits.

Positive correlations between PSII electron transport and carbon assimilation have been demonstrated under laboratory conditions, such as in *Phaseolus vulgaris* L. (Farquhar *et al.*, 1980), red campion, barley and maize (Genty *et al.*, 1989) (for review see Bellasio et al., 2016). Our climate chamber experiment also confirmed the significant positive correlation between Phi2 and carbon assimilation-related parameters (Fig. 8) across diverse inbreds of barley. In addition, significant genetic effects with high heritability were estimated for both gas exchange- and chlorophyll fluorescence-based parameters in the climate chamber (ranging from 0.76 to 0.96) (Table 3). These results show the utility of chlorophyll fluorescence-based techniques to detect genetic variation in photosynthesis under controlled conditions (Flood et al., 2016).

Despite the increasing number of studies focusing on photosynthesis under dynamic conditions (Keller *et al.*, 2019; Acevedo-Siaca *et al.*, 2021c; Fu and Walker, 2023; reviewed by Long *et al.*, 2022), few studies have demonstrated that chlorophyll fluorescence-based parameters can replace carbon assimilation parameters when investigating genetic diversity of photosynthesis parameters in the field (Bucher *et al.*, 2018). Under field conditions, in which light intensity is changing dynamically, the relationship between photosynthetic light reaction and carbon assimilation, as seen in a steady-state condition (Farquhar *et al.*, 1980; Bellasio *et al.*, 2016), may be broken (Rascher and Nedbal, 2006; Eberhard *et al.*, 2008; Long *et al.*, 2022) due to competing

processes such as photorespiration in C3 species (Pearcy, 1990; Lawson et al., 2012; Cornic and Fresneau, 2002).

However, we observed a strong positive correlation of Φ_2 between the dynamic conditions in the field and steady-state conditions in the climate chamber (Fig. 9). This correlation is based on the adjusted entry mean of Φ_2 , i.e. non-genetic variation was corrected for these means. Our results thus provide a strong support to the use of chlorophyll fluorescence-based high-throughput measurement techniques to study genetic diversity under dynamically changing, natural environmental conditions.

To use chlorophyll fluorescence-based techniques to assess highly variable photosynthesis parameters (Figs. 1 and 2) in breeding programs, however, it is important to consider the factors contributing to their variations.

Factors contributing to photosynthesis variability in the field

We observed a high variability in photosynthesis-related parameters among 23 barley inbreds in the field (Table 1, Fig. 2). Four main factors are potentially contributing to the high variability of photosynthesis-related parameters: 1) environmental conditions, 2) developmental stages, 3) genetic diversity, and 4) interaction among genotypes, environment conditions and developmental stages. Below we will discuss these factors one by one.

1) Growth environment of spring barley

We observed significant ($P < 0.05$) effects for the design variables, namely, location of the experiment, measurement date (Table 1), as well as replicate ($\sigma_{E:R}^2$). This can be explained by the dynamic environmental conditions during the growth season of spring barley, which was from late March to the beginning of August. Daily average temperature was fluctuating with an increasing trend (Supplementary Fig. 1). Also, fluctuations in light intensity occurring within and between days must have affected photosynthesis. We observed a significant ($P < 0.05$) effect of light intensity (PAR) and ambient temperature (T) (Table 2), which were considered as covariants because of the variability within a day and location of the measurement. In addition, lower

temperature in May (Supplementary Fig. 1) might have suppressed Phi2 in SEP compared to the other two developmental phases (Fig. 2B) (Bagley *et al.*, 2015; Moore *et al.*, 2021).

In parallel to the erratic changes of temperature and light intensity in the field, photosynthetic efficiency typically exhibits diurnal (Flood *et al.*, 2016) and seasonal patterns (Keller *et al.*, 2019). Leaf movement (Flood *et al.*, 2016), in interaction with dynamic environments, can also affect photosynthesis.

The significant ($P < 0.05$) variance components observed in our study for environmental factors, namely date (D), PAR and ambient temperature (T), indicate that single time point measurements are not sufficient to draw conclusions on genetic variation in photosynthesis under field conditions.

2) Developmental stages

Most previous studies exploring the genetic diversity of photosynthesis in cereals focused on carbon assimilation in the flag leaf, which is the most important leaf in pre- or post- anthesis (Driever *et al.*, 2014; Carmo-Silva *et al.*, 2017; Acevedo-Siaca *et al.*, 2021b). In our study, however, significant ($P < 0.05$) differences in photosynthesis-related parameters were observed both in the field and climate chamber experiments at different developmental stages (Figs. 2 and 7C, D) (Tables 1 and 3). As our analysis was corrected for environmental conditions, the observed differences in developmental phases are not due to the environmental changes during the experiments but due to the development of the plant itself. This is in accordance with the earlier reports of changing heritability for photosynthesis-related parameters across the lifespan of *Arabidopsis* (Flood *et al.*, 2016) and changing QTLs detected for plant growth across the cultivation period under controlled conditions (Meyer *et al.*, 2021).

Photosynthesis-related parameters are linked to plant development as well as leaf development (Wingler *et al.*, 2004; Bielczynski *et al.*, 2017). At the plant level, the sink tissues in SEP are mainly growing leaves and roots, while new sink tissues emerged in REP, such as larger root system and formation of inflorescence (Alqudah and Schnurbusch, 2017). The increased sink activity in REP coincided with the high Phi2 (Fig. 2B). In ASP, barley went from the anthesis stage to grain filling

stage, which may further increase the sink strength. However, photosynthesis-related (source) parameters did not show corresponding increases in ASP compared to REP (Fig. 2B). In fact, it has been proposed that spike photosynthesis may serve as the major photosynthesis source for grain filling, as previously shown for wheat (Maydup *et al.*, 2010; Vicente *et al.*, 2018; Molero and Reynolds, 2020).

At the leaf level, photosynthetic efficiency typically increases with leaf development to reach the maximum during leaf expansion (Bielczynski *et al.*, 2017). After anthesis, declining activity of photosynthesis has been reported in many studies (Wingler *et al.*, 2004; Liu *et al.*, 2017; Miao *et al.*, 2018; Yang *et al.*, 2018). This was not the case in the present study as no significant difference in Phi2 and SPAD was found between REP and ASP (Fig. 2B). By always choosing the top fully expanded leaves for measurements throughout all developmental stages of the plant, we minimized the effect of leaf development.

3) Genotypic effect

To evaluate the potential of classical breeding to optimize photosynthesis, the relative importance of genotypic effects versus non-genotypic effects on photosynthesis-related parameters (i.e., heritability) needs to be considered. The broad sense heritability varied between 0.16 and 0.78 (Table 1). As homozygous genotypes were evaluated in this study, dominance variance as well as additive*dominance and dominance*dominance epistasis will not contribute to the genotypic variation. Thus, broad sense heritability can be interpreted to evaluate the potential of selection.

The relatively high heritability together with the significant ($P < 0.05$) genetic variances found for Phi2, PhiNO, and qL suggests that these parameters could be manipulated in barley by photosynthesis-oriented breeding programs, hence making them promising targets for quantitative genetic approaches. Notably, the heritability of photosynthesis-related parameters varied in the different developmental stages of barley plants, with the lowest values in the seedling stage (Supplementary Fig. S3). This dynamic heritability suggests that the relative contributions of environment and genetics are not stable during the plant growth and

development (Yang *et al.*, 2015). Similar dynamic heritability of photosynthetic traits has been observed in other species, such as in field-grown wheat, in which the heritability was ranging from 0.267 to 0.764 in pre-anthesis stage and from 0.314 to 0.757 in post-anthesis stage (Carmo-Silva *et al.*, 2017). Even under controlled conditions, dynamic heritability of photosynthesis-related traits has been reported in *Arabidopsis* during long- and short-term response to light intensity (van Rooijen *et al.*, 2015; Flood *et al.*, 2016). Unlike in our study, however, the dynamic heritability found for short-term response of *Arabidopsis* under controlled conditions was mainly attributed to genetic variation and diurnal changes of photosynthesis (Flood *et al.*, 2016).

It is reasonable that the heritability of the photosynthesis-related parameters was lower in the field than that in the climate chamber (Tables 1 and 3), due to variable environmental factors and interaction between genotypes and environments (Visscher *et al.*, 2008). Given the changing heritability, taking the photosynthetic measurements when the heritability is low may not be efficient to select genotypes (Visscher *et al.*, 2008). Better knowledge about the dynamic change of heritability during plant growth and development would help us identify the developmental stage(s) when genotype significantly contributes to variation of photosynthesis, thus facilitating more targeted and efficient plant breeding (Flood *et al.*, 2016).

From an evolutionary perspective, one could argue that historical (natural or artificial) selection has reduced genotypic variance of the traits, which are more tightly associated with fitness, thus leading to a lower heritability (Mousseau and Roff, 1987; Flood, 2019). In the context of variable heritability across developmental stages of barley found in this study (Fig 3; Supplementary Fig. S3), this may imply stronger historical selection of photosynthesis in SEP than in REP, reflecting presumably the importance of the adaptation of photosynthesis in SEP (Ackerly *et al.*, 2000). Accordingly, investigating the genetics of photosynthesis-related parameters in SEP in old and therefore less selected genetic material of barley might help to understand the evolutionary pressure on photosynthesis.

4) Interactions between genotype, environment and developmental stage

As discussed above, photosynthesis is highly responsive to environmental conditions and subject to developmental influences. Except Phi2, PhiNO and qL, no significant genetic variation was observed for the other parameters. However, we found significant ($P < 0.05$) interaction effects on all photosynthesis-related parameters between genotype and environment ($G:E$), genotype and light condition ($G:L$) except Phi2 and SPAD, and genotype and developmental phases ($G:S$) except Phi2 and qL (Table 1).

The significant ($G:S$) effect suggested that the 23 inbreds showed significant different responses across the different developmental phases. This might suggest changing importance of different genes across the development phases, highlighting again the necessity to assess the genetics of photosynthesis during plant growth and development (leaf-level and plant level). While it is still challenging to assess chlorophyll fluorescence-based parameters continuously, automatically and in a high through-put fashion across plant developmental stages under field conditions, several indoor facilities are able to do this (for review see van Bezouw et al., 2019).

The significant ($G:L$) effect, on the other hand, indicates that different genes may gain importance in different light conditions. This is in line with the previous observations in *Arabidopsis* under controlled conditions (van Rooijen *et al.*, 2015; Meyer *et al.*, 2023). The separation of three light intensity levels (LL, ML, and HL) by K-means clustering (Fig. 1B), roughly corresponding to the three major phases of light response curve (Benedetti *et al.*, 2018), also underlines distinct responses of photosynthesis to different light intensity levels. In our field experiments, we could only assess the parameters of instantaneous photosynthesis while the light condition was fluctuating. However, especially in fluctuating light environments, an increasing number of studies have shown the importance of the speed of photosynthetic reactions to respond to changing light for crop yields (Kromdijk et al., 2016; De Souza et al., 2022). The relevance of natural genetic variation for such kinetic traits of photosynthesis awaits investigations.

The factors (1) – (4) are important not only in the context of photosynthesis breeding but also for fundamental understanding of how the genetics of photosynthesis interacts with environment

(E), light condition (L) and plant developmental phase (S). Quantitative knowledge and understanding of these factors are essential for improving photosynthesis models and crop yield prediction (for review see Yin and Struik, 2010)

Covariation between photosynthesis and yield-related traits

Having confirmed genetic variation for photosynthesis-related parameters in the 23 spring barley inbreds, we also analyzed the relationship between photosynthesis- and yield-related traits. The yield-related traits were collected in multi-environment and multi-year experiments, while photosynthesis-related parameters were collected in three different locations in one year. Our results indicated significant positive or negative correlations between some of the chlorophyll fluorescence parameters and NSW, but not for others (Fig. 10). The genotype*environment interactions, which are important not only for yield but also for photosynthesis, are most likely responsible for the non-significant correlations between photosynthesis-related parameters and yield-related traits in these experiments.

Several studies did not find a significant correlation between leaf-level photosynthesis and crop yields. For instance, Acevedo-Siaca *et al.* (2021a) reported no significant correlation between photosynthesis and agronomic traits of rice in field experiments. Likewise, Driever *et al.* (2014) observed no significant correlation between photosynthesis and yield in wheat. Plant growth may respond to environmental stress and perturbations more sensitively than photosynthesis does (Körner, 2015). In this case, increase in photosynthesis does not necessarily result in increased growth. Under controlled conditions or benign environments, however, targeted engineering of photosynthesis by transgenic approaches has led to increased biomass and/or yield in a number of plant species (reviewed by Simkin *et al.*, 2019). Clearly, we need to better understand the genotype*environment interactions of complex photosynthesis-related traits on one hand, and of similarly complex traits of growth and yield on the other hand to decipher the genetic relationship between photosynthesis and yield. Exploration of system biology (for review see Yin *et al.*, 2018) and gene regulatory networks (for review see Flood *et al.*, 2011; Theeuwens *et al.*, 2022) might facilitate to understand photosynthetic regulation, and how it responds to the ambient environments, which ultimately improves crop yield.

Interestingly, Φ_2 was significantly negatively correlated with flag leaf length and width across all three developmental phases (Fig. 10). This may imply that small size of flag leaf is compensated by increased photosynthetic efficiency (Poorter and Evans, 1998; Garnier *et al.*, 1999). Similar negative correlation was also observed between leaf area and CO_2 exchange rate in peanut, soybean and sweet potato (Bhagsari and Brown, 1986). Future studies may explore natural genetic variation in trait-trait interactions.

Conclusions

The results of this study show that chlorophyll fluorescence-based technique is able to detect genetic variation in PSII-related parameters in barley under climate chamber conditions, and Φ_2 , Φ_{NO} and q_L could be suitable parameters to detect genetic variation also under field conditions. Due to the significant effects of environmental factors and significant interactions between the genotype and environments, single time point measurements are not sufficient to draw conclusions on genetic variation in photosynthesis under field conditions but elaborated experimental designs are required.

Significant correlations observed between photosynthesis-related traits (F_v'/F_m' and NPQt) and yield-related traits (NSW and DMP_{FS}) in barley under field conditions suggest the possibility of improving crop yields via optimizing photosynthesis through conventional breeding approaches. Moreover, the difference in heritability of photosynthesis, across the plant development and growth stages, could be used to explore the selection pressure on photosynthesis an evolutionary timeline.

Accepted Manuscript

Table 1: Summary statistics of adjusted entry means, variance components, and broad-sense heritability (H^2) for PSII parameters and SPAD measured in the field experiments. σ_G^2 genotypic variance component; $\sigma_{G:E}^2$ variance component of interaction between genotype and environment; $\sigma_{G:L}^2$ variance component of interaction between genotype and light conditions; $\sigma_{G:S}^2$ variance component of interaction between genotype and developmental phase; σ_D^2 variance component of date of measurement, σ_M^2 variance component of MultispeQ device, $\sigma_{E:R}^2$ variance component of replicate in environment, $\sigma_{E:R:B}^2$ variance component of block nested within the replicate in environment. Note that the values of variance components of six photosynthesis-related parameters (Phi2, Fv'/Fm', PhiNO, PhiNPQ, NPQt, qL) were multiplied with 10000.

Trait	Mean	Min	Max	σ_G^2	$\sigma_{G:E}^2$	$\sigma_{G:L}^2$	$\sigma_{G:S}^2$	σ_D^2	σ_M^2	$\sigma_{E:R}^2$	$\sigma_{E:R:B}^2$	σ_e^2	H^2
LEF	126.2	110.6	139	4.987	23.742 ***	8.307 **	7.497 *	151.189 ***	236.731 ***	0.325	2.935	469.69	0.42
Phi2	0.41	0.37	0.43	0.90 ***	0.84 ***	0.17	0.24	16.25 ***	12.54 ***	0.72**	0.1	21.29	0.74
Fv'/Fm'	0.67	0.64	0.7	0.5	0.54 **	0.71***	0.87***	11.73***	2.34***	0.52**	0.03	25.52	0.58
PhiNO	0.26	0.22	0.3	1.36 ***	0.62 **	0.65 **	0.48*	6.99***	1.46 ***	1.29***	0.06	34.12	0.74
PhiNPQ	0.34	0.29	0.37	0.09	1.37 ***	0.84***	1.85***	32.62***	11.52***	0.29	0.17	32.57	0.16
NPQt	1.58	1.19	2.01	84.2	97.99***	168.23***	252.15***	1736.00***	372.24***	121.13***	7.58	5311.71	0.53
qL	0.35	0.28	0.42	4.25***	1.04*	0.96*	0	17.46***	5.51**	3.38***	0.29	83.11	0.78
SPAD	45.35	40.65	52.68	2.091	5.850 ***	0.544	5.309 ***	33.570 ***	31.471 ***	1.199 *	0.983 **	67.98	0.68

Asterisks indicate the significance of a likelihood ratio test (***, **, * indicated $P < .001, .01, .05$ respectively).

Table 2: Mean square values from analysis of variance for PSII parameters and SPAD measured in the field experiments. *G* is genotype, *PAR* is light intensity, *T* is ambient temperature, *E* is environment, *L* is light condition, *ZS* is Zadoks score of barley development, *S* is development phases.

Trait	<i>G</i>	<i>PAR</i>	<i>T</i>	<i>E</i>	<i>L</i>	<i>ZS</i>	<i>S</i>
LEF	593.67	846205.72 ***	14345.49 ***	1751.45 *	10979.05 ***	951.84	1453.20 *
Phi2	0.48 *	133.61 ***	6.99 ***	0.36	6.10 ***	0.35	1.06 **
Fv'/Fm'	0.35	29.88 ***	2.85 ***	0.09	1.00 *	4.74 ***	2.71 ***
PhiNO	0.73 *	0.04	7.99 ***	0.56	0.03	9.78 ***	5.17 ***
PhiNPQ	0.31	136.65 ***	0.23	0.12	4.93 ***	6.33 ***	2.99 ***
NPQt	69.53	5967.81 ***	264.87 *	10.22	86.6	686.60 ***	394.44 ***
qL	3.16 ***	74.74 ***	43.61 ***	0.91	4.01 **	10.01 ***	10.02 ***
SPAD	94.54	0.19	216.02	45.77	80.4	4537.56 ***	932.87 ***

Asterisks indicate the significance of a likelihood ratio test (***, **, * indicated $P < .001$, $.01$, $.05$ respectively).

Table 3: Summary statistics of adjusted entry means, variance components and broad-sense heritability (H^2) for carbon assimilation-related parameters, SPAD and PSII parameters under $1500 \mu\text{mol m}^{-2} \text{s}^{-1}$ assessed in the climate chamber experiment. σ_G^2 variance component of inbred; $\sigma_{G:S}^2$ variance component of interaction between inbred and developmental phase; σ_D^2 variance component of date of measurement, $\sigma_{D:TW}^2$ variance component of time window nested in date of measurement. Note, the values of variance components of six PSII parameters (Phi2_1500, Fv'/Fm'_1500, PhiNO_1500, PhiNPQ_1500, NPQt_1500, qL_1500) were multiplied with 100.

Trait	Mean	Min	Max	σ_G^2	$\sigma_{G:S}^2$	σ_D^2	$\sigma_{D:TW}^2$	σ_e^2	H^2
$V_{c,max}$	43.3	37.5	49.8	14.9 *	6.432 *	21.331 **	6.432 *	50.886	0.848
J_{max}	111.6	94.8	132.4	141.76 **	38.85	193.515 ***	38.85	324.241	0.895
TPU	7.61	6.37	9.13	0.717 **	0.23 *	0.688 ***	0.23	1.297	0.892
A_{sat}	17.2	14.7	19.7	2.169 *	1.32 *	2.544 **	1.319	9.608	0.82
LEF_1500	185.18	73.39	278.13	132.69 **	61.39 ***	197.73 ***	87.64 ***	707.85	0.92
Phi2_1500	0.27	0.11	0.41	0.03 **	0.01 ***	0.04 ***	0.02 ***	0.16	0.92
Fv/Fm_1500	0.6	0.21	0.75	0.05 **	0.02 **	0.05 **	0.02 **	0.26	0.92
PhiNO_1500	0.23	0.04	0.45	0.03 **	0.01	0.05 ***	0.02 *	0.27	0.86
PhiNPQ_1500	0.49	0.24	0.79	0.08 **	0.02 **	0.08 **	0.05 ***	0.39	0.93
NPQt_1500	2.33	17.89	0.64	11.70 *	5.45 **	11.51 *	6.32 **	80.99	0.9

qL_1500	0.26	0.1	0.74	0.02	0.02 *	0.11 ***	0.02 *	0.43	0.76
SPAD	44.19	6.28	75.47	36.22 ***	3.81 *	10.45	28.91 ***	75.63	0.96

Asterisks indicate the significance of a likelihood ratio test (***, **, * indicated $p_{value} \leq .001, .01, .05$ respectively).

Acknowledgement

The authors would like to thank Florian Esser and George Alskief (Institute of Quantitative Genetics and Genomics of Plants, Biology Department, Heinrich Heine University, Düsseldorf, Germany) for the field management in Cologne and Düsseldorf. We also thank Onno Muller (Institut für Bio- und Geowissenschaften (IBG), Forschungszentrum Jülich, Jülich, Germany) for organization of the field trial in Bonn. We would like to thank Urte Schlüter (Institute of Plant Biochemistry, Heinrich Heine University, Düsseldorf, Germany) for support with LI-6800. We would like to thank Katharina Luhmer (Universität Bonn, Bonn, Germany) and Monika Bilstein (Landeshauptstadt Düsseldorf, Düsseldorf, Germany) for offering the weather data. The work in BS and SM labs was supported by the DFG through the Cluster of Excellence on Plant Sciences (CEPLAS, EXC2048). WZ thanks the China Scholarship Council for a fellowship (No.202009655001). The authors thank two anonymous reviewers for helpful comments on an earlier version of the manuscript.

Declaration of Competing Interest

The authors declare that they have no known competing financial interests or personal relationships that could have appeared to influence the work reported in this paper.

Author Contribution

BS, SM conceptualized the study, acquired funding and supervised the work; YG, SM, and BS designed the research. YG, MS, LO, WZ performed experiments. YG analyzed the data. YG, SM, and BS interpreted the results. YG, SM, and BS wrote the manuscript.

Data Availability

Data are publicly available in the manuscript, and in the supplementary information.

Reference

- Acevedo-Siaca LG, Coe R, Quick WP, Long SP.** 2021a. Evaluating natural variation, heritability, and genetic advance of photosynthetic traits in rice (*Oryza sativa*). *Plant Breeding* **140**, 745–757.
- Acevedo-Siaca LG, Coe R, Quick WP, Long SP.** 2021b. Variation between rice accessions in photosynthetic induction in flag leaves and underlying mechanisms. *Journal of Experimental Botany* **72**, 1282–1294.
- Acevedo-Siaca LG, Dionora J, Laza R, Paul Quick W, Long SP.** 2021c. Dynamics of photosynthetic induction and relaxation within the canopy of rice and two wild relatives. *Food and Energy Security* **10**, 1–17.
- Ackerly DD, Dudley SA, Sultan SE, et al.** 2000. The evolution of plant ecophysiological traits: recent advances and future directions: new research addresses natural selection, genetic constraints, and the adaptive evolution of plant ecophysiological traits. *Bioscience* **50**, 979–995.
- Ainsworth EA, Serbin SP, Skoneczka JA, Townsend PA.** 2014. Using leaf optical properties to detect ozone effects on foliar biochemistry. *Photosynthesis Research* **119**, 65–76.
- Alqudah AM, Schnurbusch T.** 2017. Heading date is not flowering time in spring barley. *Frontiers in Plant Science* **8**.
- Alvarez Prado S, Gallardo JM, Serrago RA, Kruk BC, Miralles DJ.** 2013. Comparative behavior of wheat and barley associated with field release and grain weight determination. *Field Crops Research* **144**, 28–33.
- Bagley J, Rosenthal DM, Ruiz-Vera UM, Siebers MH, Kumar P, Ort DR, Bernacchi CJ.** 2015. The influence of photosynthetic acclimation to rising CO₂ and warmer temperatures on leaf and canopy photosynthesis models. *Global Biogeochemical Cycles* **29**, 194–206.
- Baker NR.** 2008. Chlorophyll fluorescence: A probe of photosynthesis in vivo. *Annual Review of Plant Biology* **59**, 89–113.
- Bellasio C, Beerling DJ, Griffiths H.** 2016. An Excel tool for deriving key photosynthetic parameters from combined gas exchange and chlorophyll fluorescence: Theory and practice. *Plant Cell and Environment* **39**, 1180–1197.
- Benedetti M, Vecchi V, Barera S, Dall'Osto L.** 2018. Biomass from microalgae: the potential of domestication towards sustainable biofactories. *Microbial Cell Factories* **17**.
- van Bezouw RF, Keurentjes JJ, Harbinson J, Aarts MG.** 2019. Converging phenomics and genomics to study natural variation in plant photosynthetic efficiency. *The Plant Journal* **97**, 112–133.
- Bhagsari AS, Brown R.** 1986. Leaf photosynthesis and its correlation with leaf area 1. *Crop science* **26**, 127–132.
- Bielczynski LW, Łacki MK, Hoefnagels I, Gambin A, Croce R.** 2017. Leaf and plant age affects photosynthetic performance and photoprotective capacity. *Plant Physiology* **175**, 1634–1648.

- Bonington S.** 1977. Climate and the efficiency of crop production in Britain. *Philosophical Transactions of the Royal Society of London. B, Biological Sciences* **281**, 277–294.
- Bucher SF, Bernhardt–Römermann M, Römermann C.** 2018. Chlorophyll fluorescence and gas exchange measurements in field research: an ecological case study. *Photosynthetica* **56**, 1161–1170.
- Carmo-Silva E, Andralojc PJ, Scales JC, Driever SM, Mead A, Lawson T, Raines CA, Parry MA.** 2017. Phenotyping of field-grown wheat in the UK highlights contribution of light response of photosynthesis and flag leaf longevity to grain yield. *Journal of Experimental Botany* **68**, 3473–3486.
- Casale F, Van Inghelandt D, Weisweiler M, Li J, Stich B.** 2022. Genomic prediction of the recombination rate variation in barley – A route to highly recombinogenic genotypes. *Plant Biotechnology Journal* **20**, 676–690.
- Cornic G, Fresneau C.** 2002. Photosynthetic Carbon Reduction and Carbon Oxidation Cycles are the Main Electron Sinks for Photosystem II Activity During a Mild Drought. *Annals of Botany* **89**, 887–894.
- De Souza AP, Burgess SJ, Doran L, Hansen J, Manukyan L, Maryn N, Gotarkar D, Leonelli L, Niyogi KK, Long SP.** 2022. Soybean photosynthesis and crop yield are improved by accelerating recovery from photoprotection. *Science* **377**, 851–854.
- Driever SM, Lawson T, Andralojc PJ, Raines CA, Parry MAJ.** 2014. Natural variation in photosynthetic capacity, growth, and yield in 64 field-grown wheat genotypes. *Journal of Experimental Botany* **65**, 4959–4973.
- Driever SM, Simkin AJ, Alotaibi S, Fisk SJ, Madgwick PJ, Sparks CA, Jones HD, Lawson T, Parry MAJ, Raines CA.** 2017. Increased sbpase activity improves photosynthesis and grain yield in wheat grown in greenhouse conditions. *Philosophical Transactions of the Royal Society B: Biological Sciences* **372**.
- Duursma RA.** 2015. Plantecophys - An R package for analysing and modelling leaf gas exchange data. *PLoS ONE* **10**, 68504.
- Eberhard S, Finazzi G, Wollman FA.** 2008. The dynamics of photosynthesis. *Annual Review of Genetics* **42**, 463–515.
- Farquhar GD, Caemmerer S, Berry JA.** 1980. A biochemical model of photosynthetic CO₂ assimilation in leaves of C₃ species. *Planta* **149**, 78–90–90.
- Flood PJ.** 2019. Using natural variation to understand the evolutionary pressures on plant photosynthesis. *Current Opinion in Plant Biology* **49**, 68–73.
- Flood PJ, Harbinson J, Aarts MGM.** 2011. Natural genetic variation in plant photosynthesis. *Trends in Plant Science* **16**, 327–335.

Flood PJ, Kruijer W, Schnabel SK, Schoor R, Jalink H, Snel JFH, Harbinson J, Aarts MGM. 2016. Phenomics for photosynthesis, growth and reflectance in *Arabidopsis thaliana* reveals circadian and long-term fluctuations in heritability. *Plant Methods* **12**, 1–14.

Fu X, Walker BJ. 2023. Dynamic response of photorespiration in fluctuating light environments. *Journal of Experimental Botany* **74**, 600–611.

Garcia A, Gaju O, Bowerman AF, Buck SA, John R, Furbank RT, Gilliam M, Millar AH, Pogson BJ. 2022. *Enhancing crop yields through improvements in the efficiency of photosynthesis and respiration.*

Garnier E, Salager J-L, Laurent G, Sonié L. 1999. Relationships between photosynthesis, nitrogen and leaf structure in 14 grass species and their dependence on the basis of expression. *The New Phytologist* **143**, 119–129.

Genty B, Briantais JM, Baker NR. 1989. The relationship between the quantum yield of photosynthetic electron transport and quenching of chlorophyll fluorescence. *Biochimica et Biophysica Acta - General Subjects* **990**, 87–92.

Gong HY, Li Y, Fang G, Hu DH, Jin WB, Wang ZH, Li YS. 2015. Transgenic rice expressing *Ictb* and *FBP/Sbpase* derived from cyanobacteria exhibits enhanced photosynthesis and mesophyll conductance to CO₂. *PLoS ONE* **10**, 1–23.

Hay WT, Bihmidine S, Mutlu N, Hoang KL, Awada T, Weeks DP, Clemente TE, Long SP. 2017. Enhancing soybean photosynthetic CO₂ assimilation using a cyanobacterial membrane protein, *ictB*. *Journal of Plant Physiology* **212**, 58–68.

Hedden P. 2003. The genes of the Green Revolution. *Trends in Genetics* **19**, 5–9.

Holland JB, Nyquist WE, Cervantes-Martínez CT, Janick J. 2003. Estimating and interpreting heritability for plant breeding: an update. *Plant breeding reviews* **22**.

Hunter MC, Smith RG, Schipanski ME, Atwood LW, Mortensen DA. 2017. Agriculture in 2050: Recalibrating targets for sustainable intensification. *BioScience* **67**, 386–391.

Kautsky H, Hirsch A. 1931. Neue Versuche zur Kohlensäureassimilation. *Naturwissenschaften* **19**, 964–964.

Keller B, Matsubara S, Rascher U, Pieruschka R, Steier A, Kraska T, Muller O. 2019. Genotype Specific Photosynthesis x Environment Interactions Captured by Automated Fluorescence Canopy Scans Over Two Fluctuating Growing Seasons. *Frontiers in Plant Science* **10**, 1–17.

Khaipho-burch M, Cooper M, Crossa J, et al. 2023. Scale up trials to validate modified crops' benefits. **621**.

Körner C. 2015. Paradigm shift in plant growth control. *Current Opinion in Plant Biology* **25**, 107–114.

Kromdijk J, Głowacka K, Leonelli L, Gabilly ST, Iwai M, Niyogi KK, Long SP. 2016. Improving photosynthesis and crop productivity by accelerating recovery from photoprotection. *Science* **354**, 857–861.

Kromdijk J, Long SP. 2016. One crop breeding cycle from starvation? How engineering crop photosynthesis for rising CO₂ and temperature could be one important route to alleviation. *Proceedings of the Royal Society B: Biological Sciences* **283**.

Kuhlgert S, Austic G, Zegarac R, et al. 2016. MultispeQ Beta: A tool for large-scale plant phenotyping connected to the open photosynQ network. *Royal Society Open Science* **3**.

Lawson T, Kramer DM, Raines CA. 2012. Improving yield by exploiting mechanisms underlying natural variation of photosynthesis. *Current Opinion in Biotechnology* **23**, 215–220.

Lithourgidis AS, Dordas CA. 2010. Forage yield, growth rate, and nitrogen uptake of faba bean intercrops with wheat, barley, and rye in three seeding ratios. *Crop Science* **50**, 2148–2158.

Liu L, Guan L, Liu X. 2017. Directly estimating diurnal changes in GPP for C₃ and C₄ crops using far-red sun-induced chlorophyll fluorescence. *Agricultural and Forest Meteorology* **232**, 1–9.

Long SP, Ainsworth EA, Leakey ADB, Nösberger J, Ort DR. 2006a. Food for thought: Lower-than-expected crop yield stimulation with rising CO₂ concentrations. *Science* **312**, 1918–1921.

Long SP, Farage PK, Garcia RL. 1996. Measurement of leaf and canopy photosynthetic CO₂ exchange in the field. *Journal of Experimental Botany* **47**, 1629–1642.

Long SP, Taylor SH, Burgess SJ, Carmo-Silva E, Lawson T, De Souza AP, Leonelli L, Wang Y. 2022. Into the Shadows and Back into Sunlight: Photosynthesis in Fluctuating Light. *Annual Review of Plant Biology* **73**, 617–648.

Long SP, Zhu XG, Naidu SL, Ort DR. 2006b. Can improvement in photosynthesis increase crop yields? *Plant, Cell and Environment* **29**, 315–330.

Maydup ML, Antonietta M, Guiamet JJ, Graciano C, López JR, Tambussi EA. 2010. The contribution of ear photosynthesis to grain filling in bread wheat (*Triticum aestivum* L.). *Field Crops Research* **119**, 48–58.

Meacham-Hensold K, Montes CM, Wu J, et al. 2019. High-throughput field phenotyping using hyperspectral reflectance and partial least squares regression (PLSR) reveals genetic modifications to photosynthetic capacity. *Remote Sensing of Environment* **231**, 111176.

Meyer RC, Weigelt-Fischer K, Knoch D, Heuermann M, Zhao Y, Altmann T. 2021. Temporal dynamics of QTL effects on vegetative growth in *Arabidopsis thaliana*. *Journal of Experimental Botany* **72**, 476–490.

Meyer RC, Weigelt-Fischer K, Tschiersch H, Topali G, Altschmied L, Heuermann MC, Knoch D, Kuhlmann M, Zhao Y, Altmann T. 2023. Dynamic growth QTL action in diverse light environments: characterization of light regime-specific and stable QTL in *Arabidopsis*. *Journal of Experimental Botany* **74**, 5341–5362.

Miao G, Guan K, Yang X, et al. 2018. Sun-induced chlorophyll fluorescence, photosynthesis, and light use efficiency of a soybean field from seasonally continuous measurements. *Journal of Geophysical Research: Biogeosciences* **123**, 610–623.

Molero G, Reynolds MP. 2020. Spike photosynthesis measured at high throughput indicates genetic variation independent of flag leaf photosynthesis. *Field Crops Research* **255**, 107866.

Moore CE, Meacham-Hensold K, Lemonnier P, Slattery RA, Benjamin C, Bernacchi CJ, Lawson T, Cavanagh AP. 2021. The effect of increasing temperature on crop photosynthesis: From enzymes to ecosystems. *Journal of Experimental Botany* **72**, 2822–2844.

Mousseau TA, Roff DA. 1987. Natural selection and the heritability of fitness components. *Heredity* **59**, 181–197.

Ogren E. 1993. Convexity of the Photosynthetic Light-Response Curve in Relation to Intensity and Direction of Light during Growth'. *Plant Physiology*, 1013–1019.

Paine CET, Marthews TR, Vogt DR, Purves D, Rees M, Hector A, Turnbull LA. 2012. How to fit nonlinear plant growth models and calculate growth rates: An update for ecologists. *Methods in Ecology and Evolution* **3**, 245–256.

Pearcy RW. 1990. Sunflecks and photosynthesis in plant canopies. *Annual review of plant biology* **41**, 421–453.

Piepho HP, Möhring J. 2007. Computing heritability and selection response from unbalanced plant breeding trials. *Genetics* **177**, 1881–1888.

Poorter H, Evans JR. 1998. Photosynthetic nitrogen-use efficiency of species that differ inherently in specific leaf area. *Oecologia* **116**, 26–37.

Prosekov AY, Ivanova SA. 2018. Food security: The challenge of the present. *Geoforum* **91**, 73–77.

Rascher U, Nedbal L. 2006. Dynamics of photosynthesis in fluctuating light. *Current Opinion in Plant Biology* **9**, 671–678.

van Rooijen R, Aarts MGM, Harbinson J. 2015. Natural genetic variation for acclimation of photosynthetic light use efficiency to growth irradiance in *Arabidopsis*. *Plant Physiology* **167**, 1412–1429.

Saathoff AJ, Welles J. 2021. Gas exchange measurements in the unsteady state. *Plant Cell and Environment* **44**, 3509–3523.

Serbin SP, Dillaway DN, Kruger EL, Townsend PA. 2011. Leaf optical properties reflect variation in photosynthetic metabolism and its sensitivity to temperature. *Journal of Experimental Botany* **63**, 489–502.

Sharkey TD. 2016. What gas exchange data can tell us about photosynthesis. *Plant Cell and Environment* **39**, 1161–1163.

- Shrestha A, Cosenza F, van Inghelandt D, Wu PY, Li J, Casale FA, Weisweiler M, Stich B.** 2022. The double round-robin population unravels the genetic architecture of grain size in barley. *Journal of Experimental Botany* **73**, 7344–7361.
- Silva-Perez V, Molero G, Serbin SP, Condon AG, Reynolds MP, Furbank RT, Evans JR.** 2017. Hyperspectral reflectance as a tool to measure biochemical and physiological traits in wheat. *Journal of Experimental Botany* **69**, 483–496.
- Simkin AJ, López-Calcagno PE, Raines CA.** 2019. Feeding the world: Improving photosynthetic efficiency for sustainable crop production. *Journal of Experimental Botany* **70**, 1119–1140.
- Theeuwens TP, Logie LL, Harbinson J, Aarts MG.** 2022. Genetics as a key to improving crop photosynthesis. *Journal of Experimental Botany* **73**, 3122–3137.
- Turnbull C, Lillemo M, Hvoslef-Eide TAK.** 2021. Global Regulation of Genetically Modified Crops Amid the Gene Edited Crop Boom – A Review. *Frontiers in Plant Science* **12**, 1–19.
- Verhulst P.** 1838. Notice on the law that the population follows in its growth. *Corresp Math Phys* **10**, 113–26.
- Vicente R, Vergara-Díaz O, Medina S, Chairi F, Kefauver SC, Bort J, Serret MD, Aparicio N, Araus JL.** 2018. Durum wheat ears perform better than the flag leaves under water stress: Gene expression and physiological evidence. *Environmental and Experimental Botany* **153**, 271–285.
- Visscher PM, Hill WG, Wray NR.** 2008. Heritability in the genomics era - Concepts and misconceptions. *Nature Reviews Genetics* **9**, 255–266.
- Ward Jr JH.** 1963. Hierarchical grouping to optimize an objective function. *Journal of the American statistical association* **58**, 236–244.
- Weisweiler M, Montaigu AD, Ries D, Pfeifer M, Stich B.** 2019. Transcriptomic and presence/absence variation in the barley genome assessed from multi-tissue mRNA sequencing and their power to predict phenotypic traits. *BMC Genomics* **20**, 1–15.
- Wingler A, Marès M, Pourtau N.** 2004. Spatial patterns and metabolic regulation of photosynthetic parameters during leaf senescence. *New Phytologist* **161**, 781–789.
- Wu PY, Stich B, Weisweiler M, Shrestha A, Erban A, Westhoff P, Inghelandt DV.** 2022. Improvement of prediction ability by integrating multi-omic datasets in barley. *BMC Genomics* **23**, 1–15.
- Wullschleger SD.** 1993. Biochemical limitations to carbon assimilation in C3 plants - a retrospective analysis of the A/Ci curves from 109 species. *Journal of Experimental Botany* **44**, 907–920.
- Yang F, Fan Y, Wu X, et al.** 2018. Auxin-to-gibberellin ratio as a signal for light intensity and quality in regulating soybean growth and matter partitioning. *Frontiers in Plant Science* **9**, 1–13.

Yang W, Guo Z, Huang C, Wang K, Jiang N, Feng H, Chen G, Liu Q, Xiong L. 2015. Genome-wide association study of rice (*Oryza sativa* L.) leaf traits with a high-throughput leaf scorer. *Journal of Experimental Botany* **66**, 5605–5615.

Yendrek CR, Tomaz T, Montes CM, Cao Y, Morse AM, Brown PJ, McIntyre LM, Leakey ADB, Ainsworth EA. 2016. High-Throughput Phenotyping of Maize Leaf Physiological and Biochemical Traits Using Hyperspectral Reflectance. *Plant Physiology* **173**, 614–626.

Yin X, van der Linden CG, Struik PC. 2018. Bringing genetics and biochemistry to crop modelling, and vice versa. *European Journal of Agronomy* **100**, 132–140.

Yin X, Struik PC. 2010. Modelling the crop: from system dynamics to systems biology. *Journal of Experimental Botany* **61**, 2171–2183.

Zadoks JC, Chang TT, Konzak CF. 1974. A decimal code for the growth stages of cereals. *Weed Research* **14**, 415–421.

Zhu XG, Long SP, Ort DR. 2010. Improving photosynthetic efficiency for greater yield. *Annual Review of Plant Biology* **61**, 235–261.

Accepted Manuscript

Figure legends.

Fig.1 Liner electron flow (LEF) for 23 barley inbred lines in the field experiment in response to changing light intensity across all environments. The different colors of the dots in (A) indicate 23 different barley inbred lines. Three different colors of the dots in (B) represent the clusters of low (LL), medium (ML) and high (HL) light condition.

Fig.2: Effects of light intensity and developmental phase on the quantum yield of PSII (Φ_2), the quantum yield of non-photochemical quenching (Φ_{NPQ}) and relative chlorophyll content (SPAD) of 23 barley inbred lines. (A) Comparison of three light conditions: LL (low light), ML (medium light), and HL (high light). (B) Comparison of three developmental phases: SEP (slow expansive phase; Zadoks score, ZS, from 10 to 29), REP (rapid expansive phase; ZS from 30 to 59), and ASP (anthesis and senescence phase; ZS from 60 to 87). The colored dots represent the adjusted entry means for 23 barley inbred lines. The red point next to each box plot indicates the average across all inbreds for each light condition (A) or developmental phase (B). The letters next to each box plot indicate statistical significance. Different letters denote significant differences based on Tukey-test ($P < 0.05$) between the means for each parameter in each condition.

Fig.3: Heritability of PSII parameters and SPAD in different developmental phases. SEP: Slow expansive phase (Zadoks score (ZS) from 10 to 29); REP: Rapid expansive phase (ZS from 30 to 59); ASP: Anthesis and senescence phase (ZS from 60 to 87). The red point next to each box plot indicates the mean heritability across all traits for each developmental phase. Different letters next to each box plot indicate significant differences based on Tukey-test ($P < 0.05$) between the mean heritability.

Fig.4: Hierarchical clustering (A) of 23 barley inbred lines based on their adjusted entry means for PSII parameters and SPAD in three developmental phases, principal component analysis (B) based on the adjusted entry means of the combination of PSII parameters and SPAD in three developmental phases, the growth-related parameters based on dry mass per plant, and the morphological traits from multi-year and multi-environment experiments, and person correlation coefficients (C) calculated between pairs of PC1 and PC2 loadings of each inbred in PCA (B), precipitation and temperature of the country of the origin of each inbred.

Fig. 5: Comparison of PSII parameters, SPAD and growth-related parameters among the four clusters. (A) PSII parameters and SPAD in different developmental phases. (B) Dry mass per plant (DMP) and relative growth rates (RGR_a , RGR_b , RGR_c) calculated from DMP based on the

quadratic regression ($y_r = a + bt - ct^2$). Due to the wide range of RGR_c , log-transformed data of RGR_c was used. The red point next to each box plot indicates the mean of the parameters in each cluster. Different letters next to each box show significant differences based on Tukey-test ($P < 0.05$) between the clusters.

Fig.6: Person correlation coefficients calculated between pairs of adjusted entry means of 23 barley inbreds for photosynthesis- and growth-related parameters collected in the field. Asterisks indicate the significance level (***, **, * indicated $P < .001, .01, .05$ respectively).

Fig.7: Comparison of the six barley inbred lines in the climate chamber. (A) Carbon assimilation-related parameters (A_{sat} , $V_{c,max}$, J_{max} , TPU). (B) Phi2 under simulated LL (PAR 400 $\mu\text{mol m}^{-2} \text{s}^{-1}$), ML (800 $\mu\text{mol m}^{-2} \text{s}^{-1}$), and HL (1500 $\mu\text{mol m}^{-2} \text{s}^{-1}$) conditions, and SPAD. For (A) and (B), the colors of boxes represent the clusters determined by the hierarchical clustering in Fig. 5a. (C) Adjusted entry means of A_{sat} , $V_{c,max}$, J_{max} , TPU of the six inbred lines in SEP, REP, and ASP. (D) Adjusted entry means of Phi2 under the simulated LL, ML, and HL conditions, and SPAD of the six inbred lines in different developmental phases. The red dots next to boxes in (A) and (B) are the adjusted entry means of parameters of each genotype. The red dots next to boxes in (C) and (D) are the mean values of the six inbreds for each parameter in each developmental phase. Different letters next to each box denote significant difference based on Tukey-test ($P < 0.05$).

Fig.8: Person correlation coefficients calculated between pairs of adjusted entry means for six barley inbreds for photosynthesis-related parameters, dry mass per plant, harvest index (HI), flag leaf width (FW), flag leaf length (FL), flag leaf area (FA) and relative growth rate related parameters (RGR_a , RGR_b , RGR_c), awn length (AL), spike length (EL), and spikelet number in one row of the spike (SR), seed length (SL), seed width (SW) seed area (SA) and thousand grain weight (TGW), total aboveground dry mass (DMP), total stem weight without spike weight (SWP), harvest index (HI), spike weight per plant (SKWP), main stem harvest index (MSHI) which were collected from the climate chamber experiments. Asterisks indicate the significance level (***, **, * indicated $P < .001, .01, .05$ respectively).

Fig. 9: Person correlation coefficients calculated between pairs of adjusted entry means of six barley inbreds for Phi2 and carbon assimilation-related parameters measured in the climate chamber experiments (CE) and Phi2 measured in the field (FE). Phi2 was assessed separately for LL, ML and HL conditions. Carbon assimilation was analysed at the light intensity of the HL condition. Asterisks indicate the significance level (***, **, * indicated $P < .001, .01, .05$ respectively).

*Fig. 10: Person correlation coefficients calculated between pairs of adjusted entry means of 23 barley inbreds for PSII parameters, SPAD and morphological traits collected from multiple environments and years in the field conditions. Asterisks indicate the significance level (***, **, * indicated $P < .001, .01, .05$ respectively)*

Accepted Manuscript

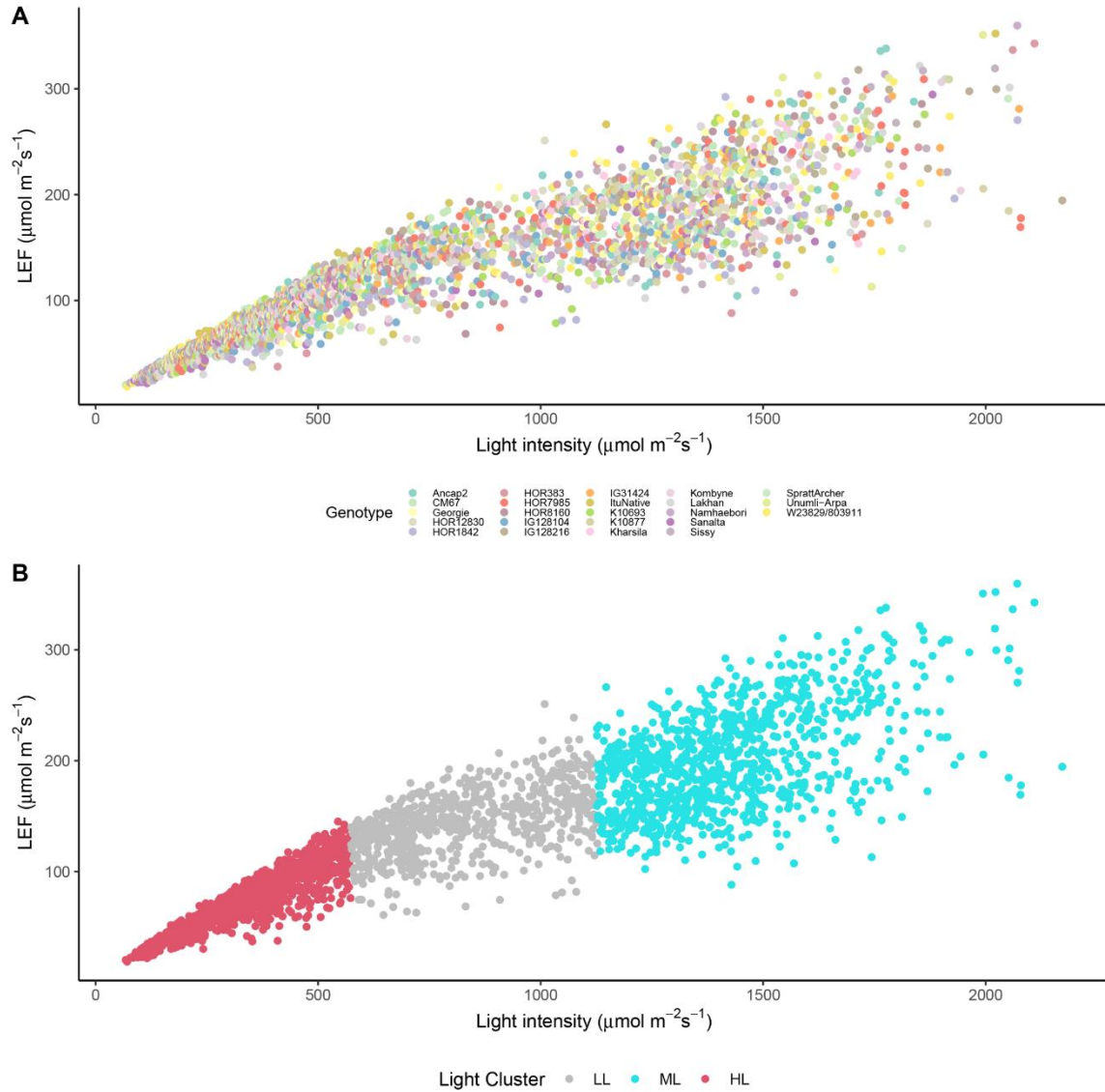


Fig.1 Liner electron flow (LEF) for 23 barley inbred lines in the field experiment in response to changing light intensity across all environments. The different colors of the dots in (A) indicate 23 different barley inbred lines. Three different colors of the dots in (B) represent the clusters of low (LL), medium (ML) and high (HL) light condition.



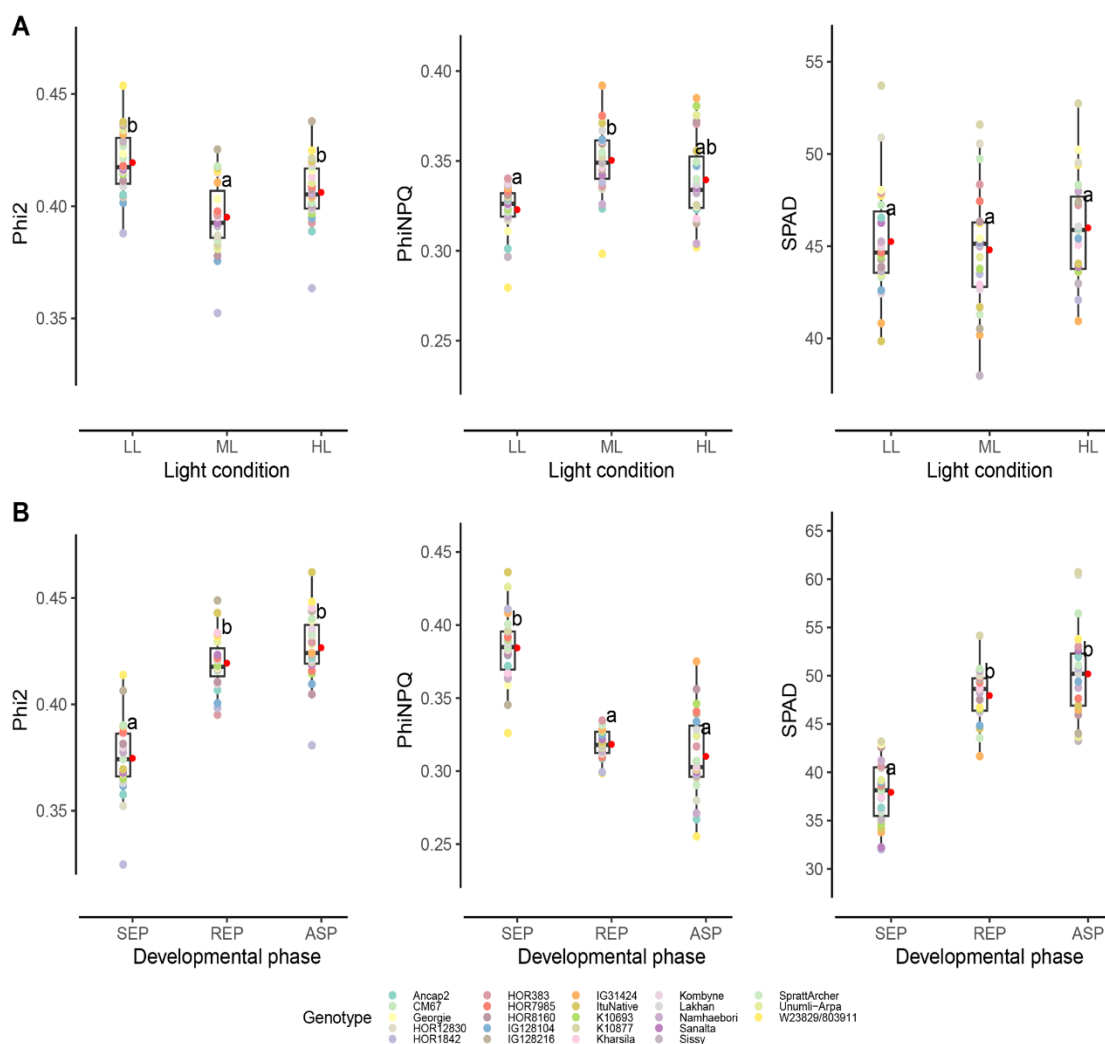


Fig.2 Effects of light intensity and developmental phase on the quantum yield of PSII (Phi2), the quantum yield of non-photochemical quenching (PhiNPQ) and relative chlorophyll content (SPAD) of 23 barley inbred lines. (A) Comparison of three light conditions: LL (low light), ML (medium light), and HL (high light). (B) Comparison of three developmental phases: SEP (slow expansive phase; Zadoks score, ZS, from 10 to 29), REP (rapid expansive phase; ZS from 30 to 59), and ASP (anthesis and senescence phase; ZS from 60 to 87). The colored dots represent the adjusted entry means for 23 barley inbred lines. The red point next to each box plot indicates the average across all inbreds for each light condition (A) or developmental phase (B). The letters next to each box plot indicate statistical significance. Different letters denote significant differences based on Tukey-test ($P < 0.05$) between the means for each parameter in each condition.

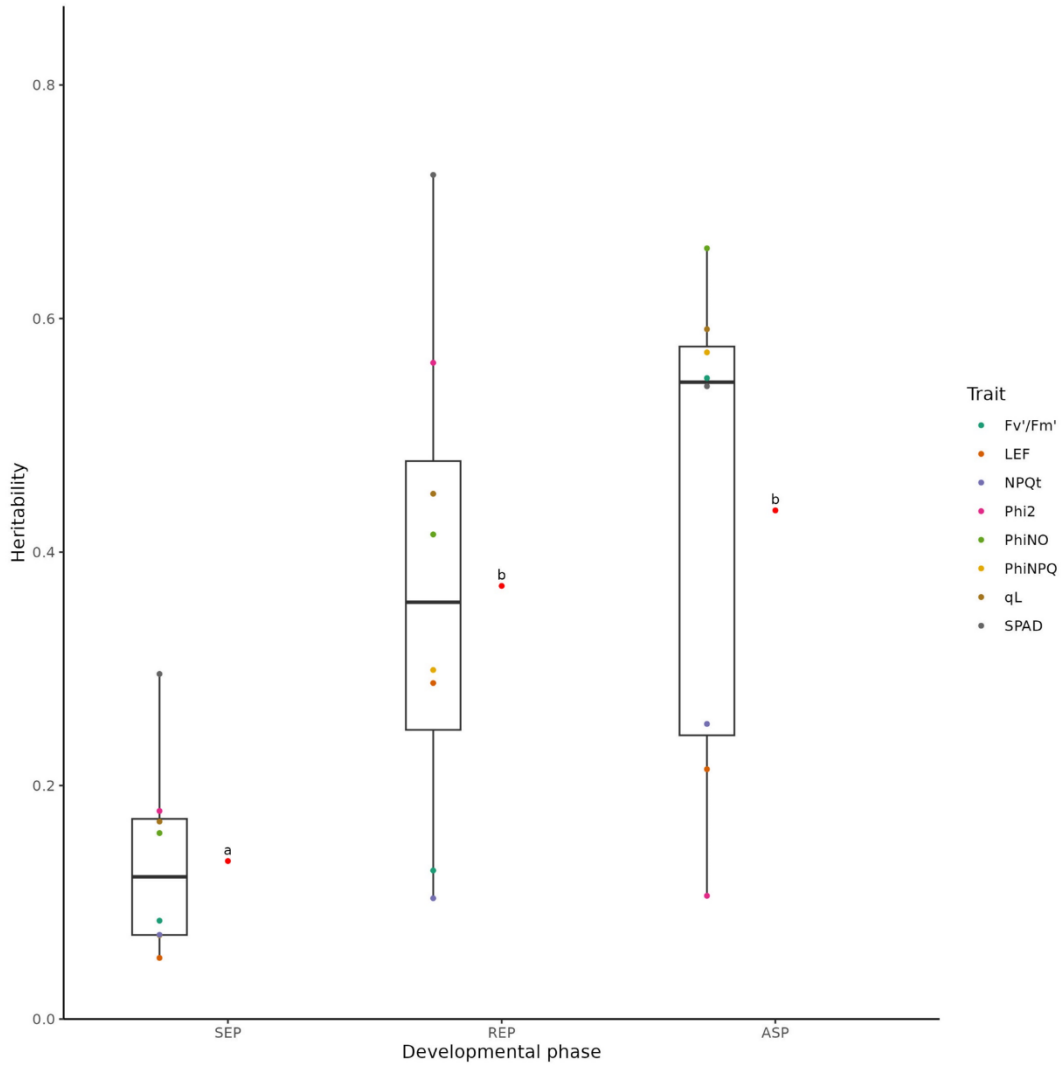


Fig.3 Heritability of PSII parameters and SPAD in different developmental phases. SEP: Slow expansive phase (Zadoks score (ZS) from 10 to 29); REP: Rapid expansive phase (ZS from 30 to 59); ASP: Anthesis and senescence phase (ZS from 60 to 87). The red point next to each box plot indicates the mean heritability across all traits for each developmental phase. Different letters next to each box plot indicate significant differences based on Tukey-test ($P < 0.05$) between the mean heritability

A

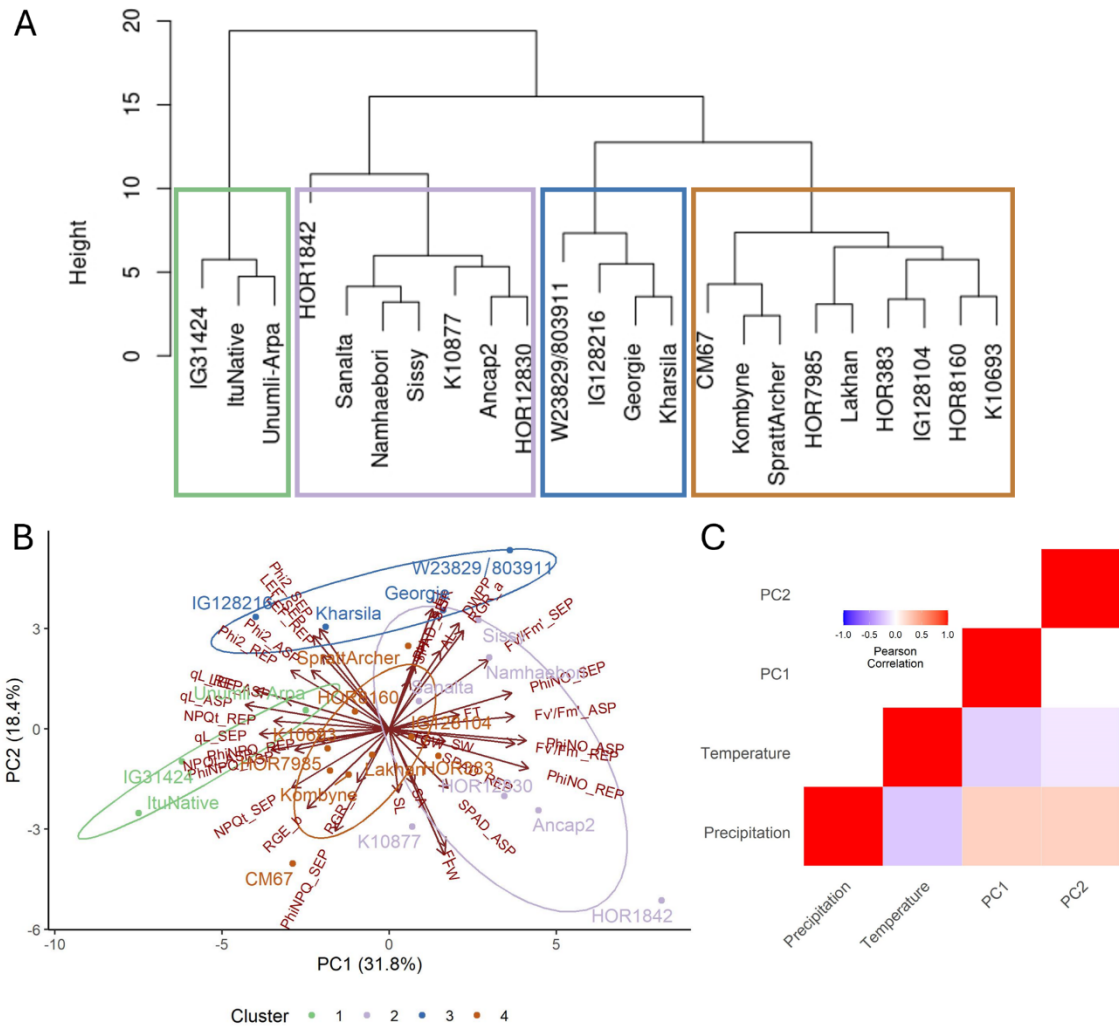


Fig.4 Hierarchical clustering (A) of 23 barley inbred lines based on their adjusted entry means for PSII parameters and SPAD in three developmental phases, principal component analysis (B) based on the adjusted entry means of the combination of PSII parameters and SPAD in three developmental phases, the growth-related parameters based on dry mass per plant, and the morphological traits from multi-year and multi-environment experiments, and person correlation coefficients (C) calculated between pairs of PC1 and PC2 loadings of each inbred in PCA (B), precipitation and temperature of the country of the origin of each inbred.

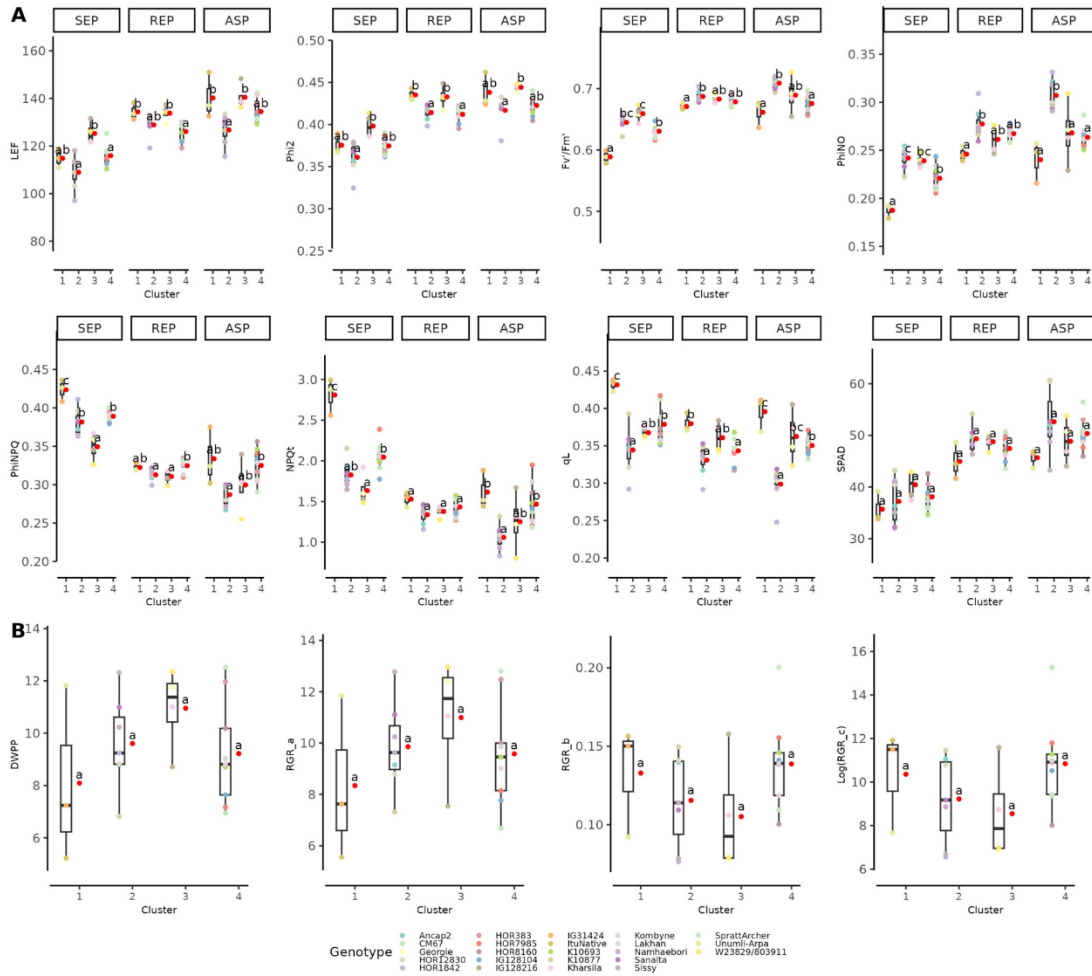


Fig.5 Comparison of PSII parameters, SPAD and growth-related parameters among the four clusters. (A) PSII parameters and SPAD in different developmental phases. (B) Dry mass per plant (DMP) and relative growth rates (RGR_a, RGR_b, RGR_c) calculated from DMP based on the quadratic regression ($y_T = a + bt - ct^2$). Due to the wide range of RGR_c, log-transformed data of RGR_c was used. The red point next to each box plot indicates the mean of the parameters in each cluster. Different letters next to each box show significant differences based on Tukey-test ($P < 0.05$) between the clusters.

AC

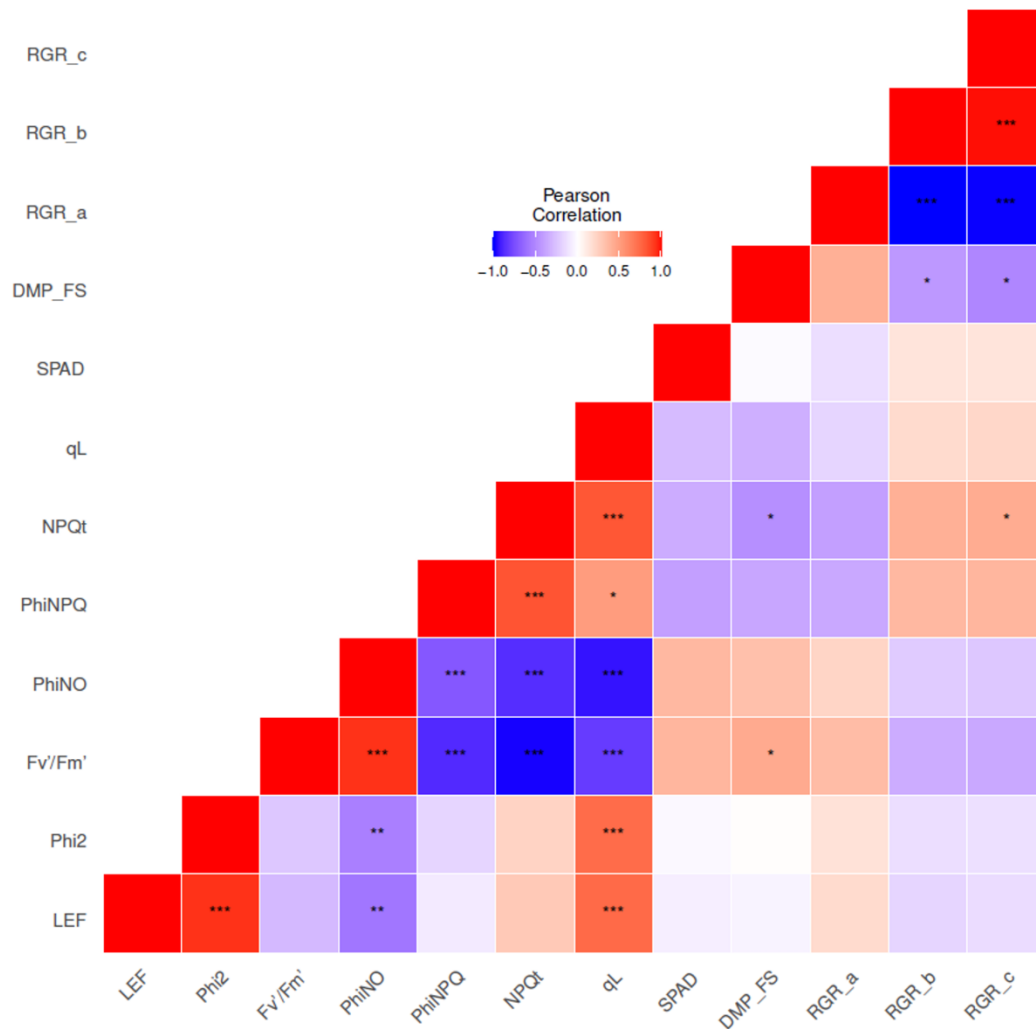


Fig.6 Person correlation coefficients calculated between pairs of adjusted entry means of 23 barley inbreds for photosynthesis- and growth-related parameters collected in the field. Asterisks indicate the significance level (***, **, * indicated $P < .001$, $.01$, $.05$ respectively).

ACCEPTED

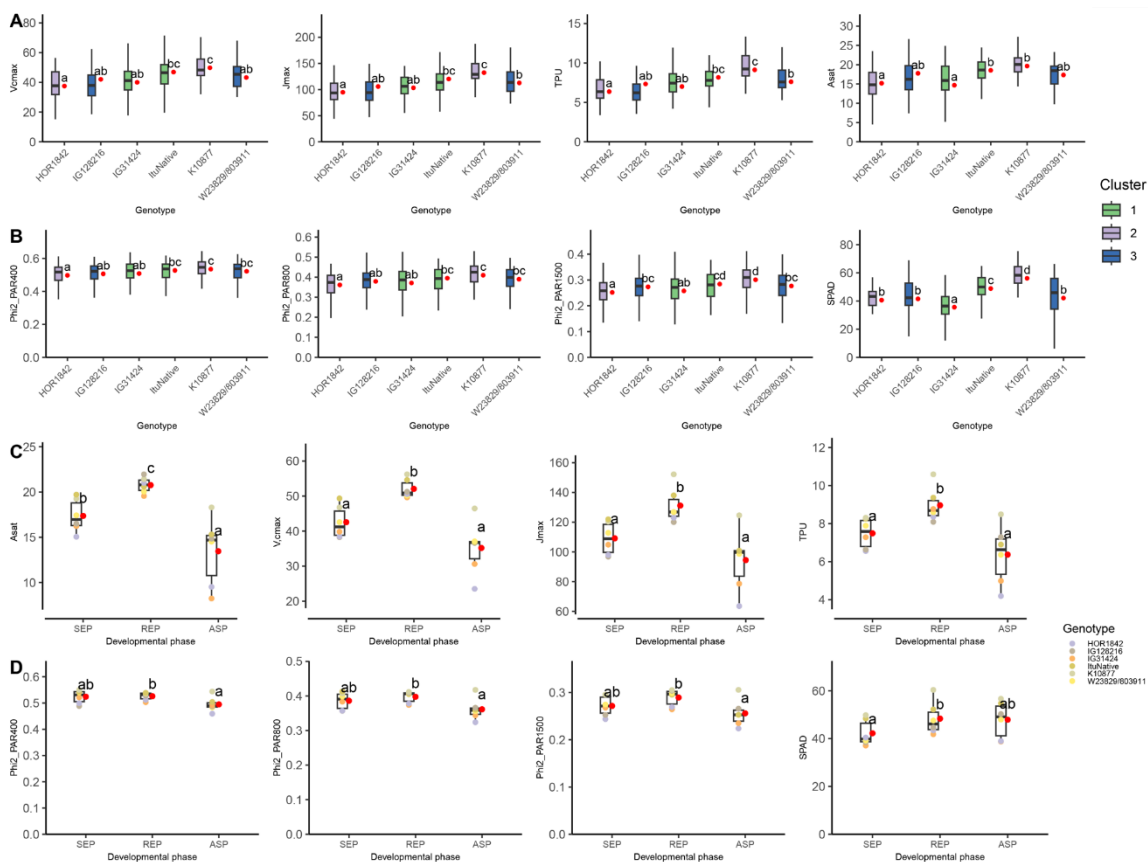


Fig.7 Comparison of the six barley inbred lines in the climate chamber. (A) Carbon assimilation-related parameters (A_{sat} , $V_{c,max}$, J_{max} , TPU). (B) Φ_2 under simulated LL (PAR 400 $\mu\text{mol m}^{-2} \text{s}^{-1}$), ML (800 $\mu\text{mol m}^{-2} \text{s}^{-1}$), and HL (1500 $\mu\text{mol m}^{-2} \text{s}^{-1}$) conditions, and SPAD. For (A) and (B), the colors of boxes represent the clusters determined by the hierarchical clustering in Fig. 5a. (C) Adjusted entry means of A_{sat} , $V_{c,max}$, J_{max} , TPU of the six inbred lines in SEP, REP, and ASP. (D) Adjusted entry means of Φ_2 under the simulated LL, ML, and HL conditions, and SPAD of the six inbred lines in different developmental phases. The red dots next to boxes in (A) and (B) are the adjusted entry means of parameters of each genotype. The red dots next to boxes in (C) and (D) are the mean values of the six inbreds for each parameter in each developmental phase. Different letters next to each box denote significant difference based on Tukey-test ($P < 0.05$).

ACQ

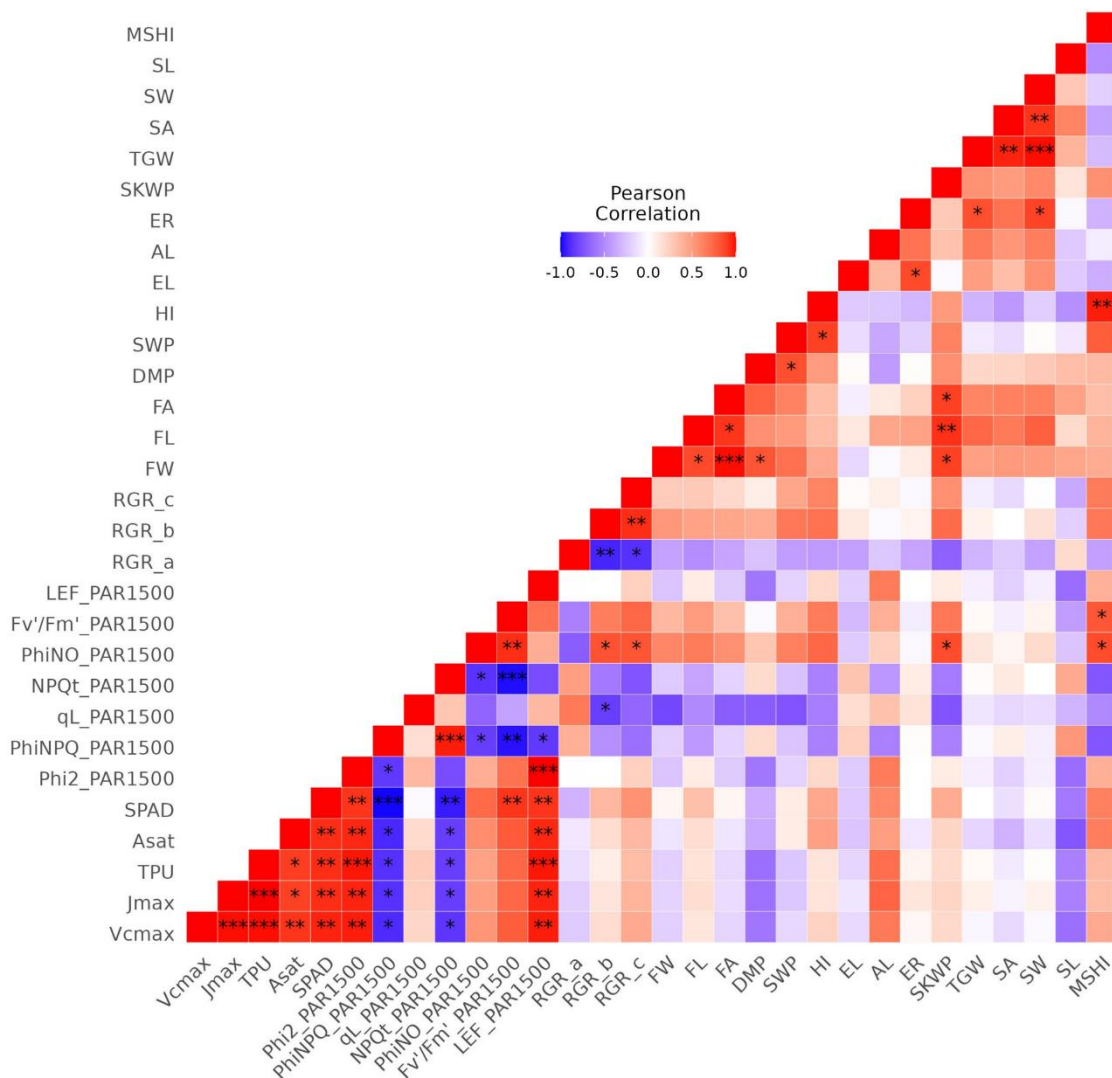


Fig.8 Person correlation coefficients calculated between pairs of adjusted entry means for six barley inbreds for photosynthesis-related parameters, dry mass per plant, harvest index (HI), flag leaf width (FW), flag leaf length (FL), flag leaf area (FA) and relative growth rate related parameters (RGR_a, RGR_b, RGR_c), awn length (AL), spike length (EL), and spikelet number in one row of the spike (SR), seed length (SL), seed width (SW) seed area (SA) and thousand grain weight (TGW), total aboveground dry mass (DMP), total stem weight without spike weight (SWP), harvest index (HI), spike weight per plant (SKWP), main stem harvest index (MSHI) which were collected from the climate chamber experiments. Asterisks indicate the significance level (***, **, * indicated $P < .001, .01, .05$ respectively).

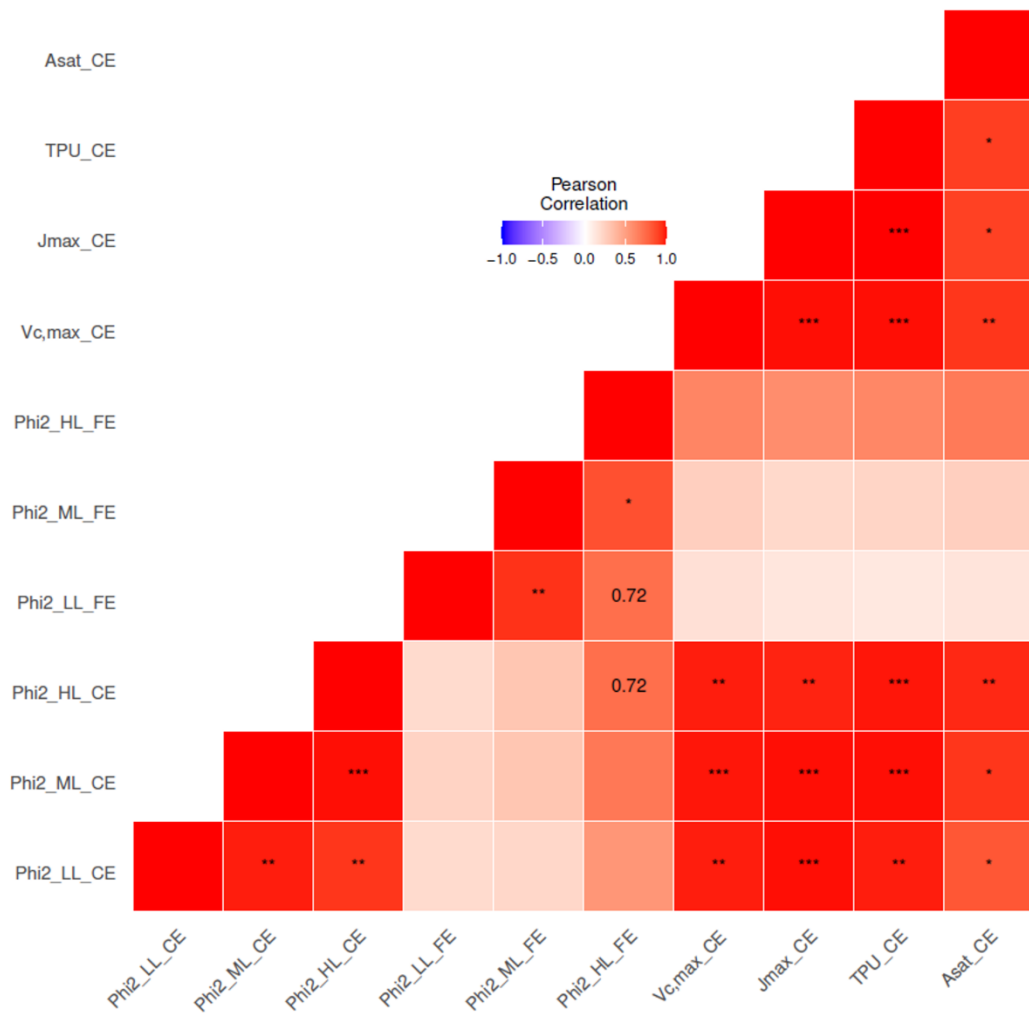


Fig.9 Pearson correlation coefficients calculated between pairs of adjusted entry means of six barley inbreds for Phi2 and carbon assimilation-related parameters measured in the climate chamber experiments (CE) and Phi2 measured in the field (FE). Phi2 was assessed separately for LL, ML and HL conditions. Carbon assimilation was analyzed at the light intensity of the HL condition. Asterisks indicate the significance level (***, **, * indicated $P < .001, .01, .05$ respectively).

AC

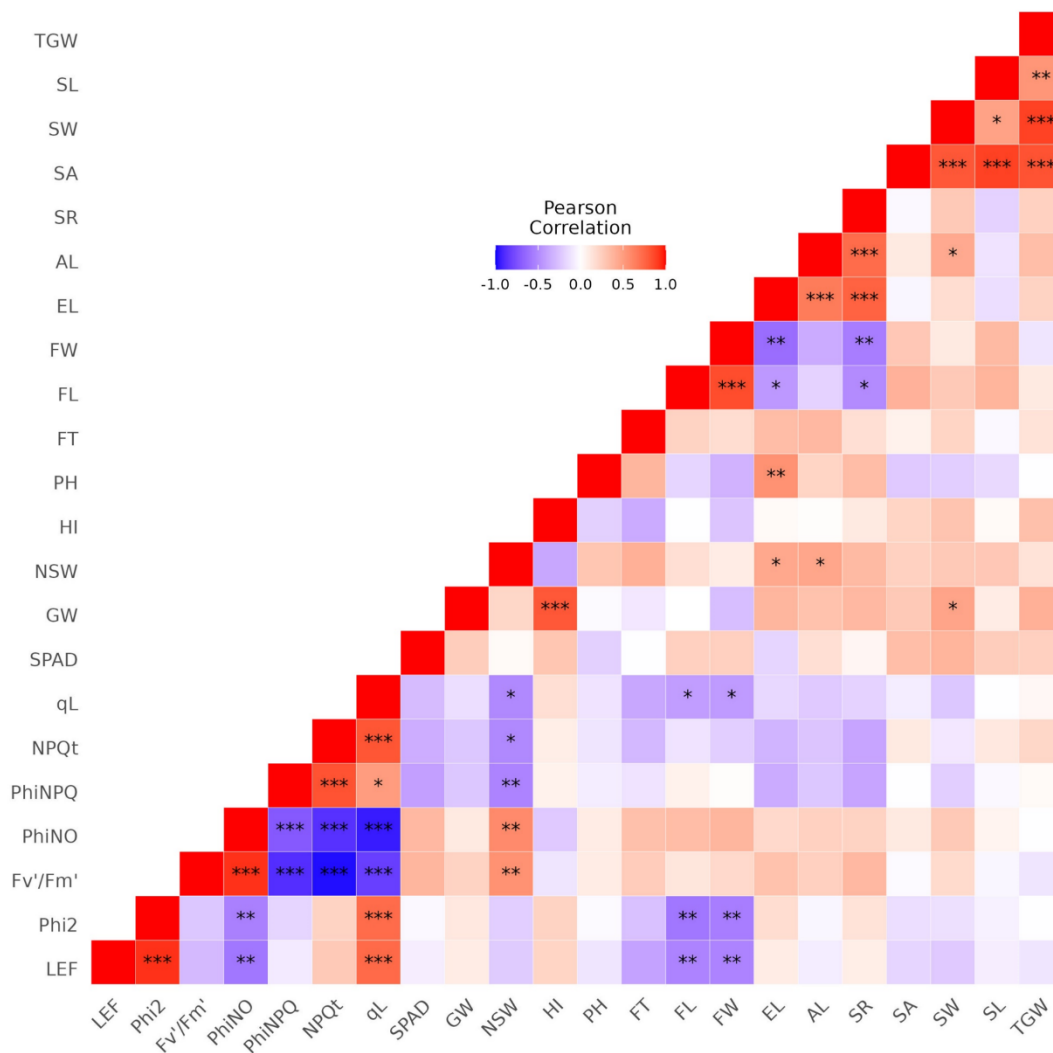


Fig.10 Person correlation coefficients calculated between pairs of adjusted entry means of 23 barley inbreds for PSII parameters, SPAD and morphological traits collected from multiple environments and years in the field conditions. Asterisks indicate the significance level (***, **, * indicated P < .001, .01, .05 respectively)

AC